

# Experimental investigation into the effects of cast-iron pipe corrosion on GPR detection performance in clay soils

Moghareh Abed, Tara; Eskandari Torbaghan, Mehran; Hojjati, Aryan; Rogers, Christopher D.F.; Chapman, David N.

DOI:

[10.1061/\(ASCE\)PS.1949-1204.0000491](https://doi.org/10.1061/(ASCE)PS.1949-1204.0000491)

License:

Other (please specify with Rights Statement)

*Document Version*

Peer reviewed version

*Citation for published version (Harvard):*

Moghareh Abed, T, Eskandari Torbaghan, M, Hojjati, A, Rogers, CDF & Chapman, DN 2020, 'Experimental investigation into the effects of cast-iron pipe corrosion on GPR detection performance in clay soils', *Pipeline System Engineering and Practice*, vol. 11, no. 4, 04020040. [https://doi.org/10.1061/\(ASCE\)PS.1949-1204.0000491](https://doi.org/10.1061/(ASCE)PS.1949-1204.0000491)

[Link to publication on Research at Birmingham portal](#)

## **Publisher Rights Statement:**

This material may be downloaded for personal use only. Any other use requires prior permission of the American Society of Civil Engineers. This material may be found at: [https://doi.org/10.1061/\(ASCE\)PS.1949-1204.0000491](https://doi.org/10.1061/(ASCE)PS.1949-1204.0000491)

## **General rights**

Unless a licence is specified above, all rights (including copyright and moral rights) in this document are retained by the authors and/or the copyright holders. The express permission of the copyright holder must be obtained for any use of this material other than for purposes permitted by law.

- Users may freely distribute the URL that is used to identify this publication.
- Users may download and/or print one copy of the publication from the University of Birmingham research portal for the purpose of private study or non-commercial research.
- User may use extracts from the document in line with the concept of 'fair dealing' under the Copyright, Designs and Patents Act 1988 (?)
- Users may not further distribute the material nor use it for the purposes of commercial gain.

Where a licence is displayed above, please note the terms and conditions of the licence govern your use of this document.

When citing, please reference the published version.

## **Take down policy**

While the University of Birmingham exercises care and attention in making items available there are rare occasions when an item has been uploaded in error or has been deemed to be commercially or otherwise sensitive.

If you believe that this is the case for this document, please contact [UBIRA@lists.bham.ac.uk](mailto:UBIRA@lists.bham.ac.uk) providing details and we will remove access to the work immediately and investigate.

Article type: Research Paper

# Title: An Experimental Investigation into the Effects of Cast Iron Pipe Corrosion on GPR Detection Performance in Clay Soils

Author 1

- **Given name:** Tara **Family name:** Moghareh Abed, BSc, MSc, PhD.
- Shalini Misra Ltd, Shalini Misra, 4b Lonsdale Rd, Queen's Park, London NW6 6RD, E-Mail: [txm712@bham.ac.uk](mailto:txm712@bham.ac.uk)

Author 2 (Corresponding author)

- **Given name:** Mehran **Family name:** Eskandari Torbaghan, BSc, MSc, PhD, MCIHT Research Fellow
- School of Engineering, Department of Civil Engineering, College of Engineering and Physical Sciences, University of Birmingham, Birmingham, B15 2TT, UK, Tel.: +44-74056-39382, E-Mail: [m.eskandaritorbaghan@bham.ac.uk](mailto:m.eskandaritorbaghan@bham.ac.uk)

Author 3

- **Given name:** Aryan **Family name:** Hojjati, MEng, GMICE, AFHEA, Research Fellow
- School of Engineering, Department of Civil Engineering, College of Engineering and Physical Sciences, University of Birmingham, Birmingham, B15 2TT, UK. Tel.: +44 121 414 3564 E-Mail: [a.hojjati@bham.ac.uk](mailto:a.hojjati@bham.ac.uk)

Author 4

- **Given name:** Christopher D.F. **Family name:** Rogers, Professor of Geotechnical Engineering, Eur Ing, BSc, PhD, CEng, MICE, MCIHT
- School of Engineering, Department of Civil Engineering, College of Engineering and Physical Sciences, University of Birmingham, Birmingham, B15 2TT, UK, Tel.: +44 (0) 121 414 5066, Email: [c.d.f.rogers@bham.ac.uk](mailto:c.d.f.rogers@bham.ac.uk)

Author 5

- **Given name:** David N. **Family name:** Chapman, Professor of Geotechnical Engineering, BSc (Hons), DIS, PhD, CEng, MICE, FHEA
- School of Engineering, Department of Civil Engineering, College of Engineering and Physical Sciences, University of Birmingham, Birmingham, B15 2TT, UK, Tel.: +44 (0) 121 414 5150, Email: [d.n.chapman@bham.ac.uk](mailto:d.n.chapman@bham.ac.uk)

## **Abstract**

Cast iron water distribution pipes are used widely in the UK and worldwide. Corrosion of these cast iron pipes often occurs due to an electrochemical process where the pipe is buried directly in a chemically aggressive ground (as is the case for some clays). The electrochemical process changes the pH environment and releases iron ions into the clay. This can cause chemical alteration of the clay minerals and ‘corrosion products’, such as iron oxide, hydroxide and aqueous salts, to form in the soil. These chemical interactions are complex and time dependent, and can potentially result in pipe failure, and thus the conditions under which they occur need to be understood.

Ground Penetrating Radar (GPR) has been proposed for routinely detecting, assessing and monitoring buried cast iron pipes, and thus it is important to know how these chemical changes affect the electromagnetic properties of soil. A bespoke set of laboratory experiments was devised to simulate and accelerate cast iron corrosion (using electrokinetics) and ion migration processes in two types of clay, namely Kaolin Clay and Oxford Clay. Tests were conducted for periods of up to 3 months using both inert electrodes and a cast iron disc as the anode. The changes in the geotechnical properties (undrained shear strength, moisture content and Atterberg limits), the geophysical properties (permittivity) and the geochemical properties (iron content, pH and conductivity) were monitored. The results indicated that the Oxford Clay was much more aggressive in terms of the corrosion activity compared to the Kaolin Clay. The laboratory results were used in GPR simulations in relation to the detection of a buried cast iron pipe. The results showed that the chemically induced changes to the Kaolin Clay did not materially affect the performance of GPR to detect the cast iron pipe, whereas a pipe buried in Oxford Clay the (greatly accelerated) chemically-induced changes were sufficiently advanced after approximately 7-8 weeks to cause the GPR to be unable to detect the corroded pipe.

## **Keywords**

cast iron pipe; corrosion; geotechnical properties; geophysical properties; geochemical properties; Ground Penetrating Radar (GPR) modelling

## **Abbreviations**

BSI                British Standards Institution

EC                Electrical Conductivity

67	EK	Electrokinetic
68	FDTD	Finite Difference Time Domain
69	GPR	Ground Penetrating Radar
70	NDT	Non-Destructive Technologies
71	pH	Acidity / Alkalinity of system / $-\log_{10}$ of hydrogen ions activity
72	PVC	Polyvinyl Chloride
73	TDR	Time-Domain Reflectometry
74	USS	Undrained Shear Strength
75	Vp	Propagation Velocity

## 76    **1    Introduction**

77    Cast iron pipes have been widely used for transferring potable water, being routinely used from  
78    the early 1800s, particularly in the USA, (Merdinger, 1955), and extensively used to build  
79    water distribution systems in the UK, to the extent that it was called the ‘wonder material of  
80    the Victorian era’ (Gagg and Lewis, 2011). Its use continued until ductile iron pipes were  
81    introduced in the 1970s (Rajani *et al.*, 1996). Nevertheless, cast iron is still the most common  
82    material found in existing pipes, and is also the material that produces the highest number of  
83    bursts historically (Marshall, 2001; Makar and McDonald, 2007; Folkman, 2018). The most  
84    common corrosion failure mechanism for buried cast iron pipes is localised corrosion, which  
85    can lead to leakage (WSAA, 2003). It has been found that cast iron pipes have a very high  
86    failure rate in some particular soils, i.e. in soils that are particularly aggressive such as London  
87    Clay (Schmidt, 2007). This suggests an involvement of chemical processes, in addition to  
88    mechanical deterioration mechanisms (London Clay is also active in terms of shrinkage and  
89    swelling behaviour), induced by the prevailing environmental conditions (Bradford, 2000).  
90    Cast iron pipe corrosion occurs readily in saturated or partially-saturated zones of clays, where  
91    electrochemical oxidation takes place in the presence of oxygenated water. This is called  
92    graphitic corrosion and is caused by the creation of a galvanic cell between the cast iron (the  
93    anode, where the pH is lowered) and the surrounding high-conductivity clay (the cathode)  
94    (Freeman, 1999). Buried pipes are in direct contact with the soil, with different physical and

geochemical properties, and therefore the prevalence for corrosion to occur can change over the length of a pipe.

Cast iron corrosion in soil occurs due to electrochemical processes and results in the formation of pitting, converting metal substrates to oxides, hydroxides and aqueous salts (in anode-cathode systems) (Romanoff, 1964). These corrosion products are released into the surrounding soil, changing the chemical, geotechnical and geophysical properties of the soil, although the interactions between these properties are not well understood (Figure 1). The release of ions from a corroding buried iron pipe is expected to increase the rate of pipe corrosion due to an increase in ion concentrations in the surrounding soil (Ekine and Emujakporue, 2010). These released ions contaminate the surrounding soil, elevating the iron/cation content and creating a diffuse plume zone around the source, i.e. the cast iron pipe (Yong and Mulligan, 2003). The plume zone is where ion diffusion and migration occur, and this can ultimately lead to modification of the soil, with the concentration of these ion contaminants decreasing away from the cast iron pipe as they form precipitates or complexes with the surrounding soil (Yong and Mulligan, 2003).

Routine and yet effective condition assessment of these buried pipes can minimise the negative consequences of deterioration in the utility network. To further minimise the risk of damaging the utility network adopting non-destructive technologies (NDT) for assessment would be ideal as they have the potential for providing routine and effective assessment with minimum disruption (Roberge, 2007; Rainer *et al.*, 2017). Geophysical techniques, such as Ground Penetrating Radar (GPR), have been utilised to locate and map cast iron pipes (Mooney *et al.*, 2010; Pennock *et al.*, 2010; Ayala-Cabrera *et al.*, 2011) and assess their condition (Hao *et al.*, 2012; Liu *et al.*, 2012; Rogers *et al.*, 2012; Liu and Kleiner, 2013) including determination of the corroded state of cast iron pipes. Having said that, as it is suggested in the literature, e.g. (Pennock *et al.*, 2010), chemical alteration of fine-grained soil by cast iron corrosion products may inhibit GPR's abilities to be used for utility mapping or assessment.

The aim of this paper is to investigate the effects of the corrosion of buried cast iron pipes on the geophysical, geochemical and electromagnetic properties of the surrounding clay soils, as these soils are known to be aggressive towards buried metals (Bonds *et al.*, 2005; Veleva, 2005; Cole and Marney, 2012), and hence to explore the reported tendency of deteriorated cast iron pipes being harder to detect using GPR than pristine pipes. This has been done through controlled laboratory experiments that simulate the corrosion and ion migration process.

## 2 GPR Application for Iron Pipe Condition Assessment

Over the last two decades, a number of different NDTs have been utilised for inspecting water pipes, including seismic and acoustic methods (Demma *et al.*, 2004; Choi *et al.*, 2017) and infrared thermography (Bach and Kodikara, 2017). Some of these NDT technologies exploit specific pipe materials properties, and consequently they are not suitable for use with all pipe materials (Atef, 2010). However, the GPR technique has been widely used for shallow geophysical investigation (Costello *et al.*, 2007; Demirci *et al.*, 2012). Its main advantage is that it can survey large areas at a speed that makes real time interpretation possible. In this method an electromagnetic wave (generally between 1 MHz to 1 GHz) is transmitted through the ground and the Time-of-Flight (ToF) from the reflected wave is measured (Metje *et al.*, 2007). GPR has been used for investigating and monitoring underground water, locating wet patches, and hence pipe leaks, e.g. Tran and Lambot (2015); Algeo *et al.* (2016); Fedorova *et al.* (2016). Algeo *et al.* (2016) successfully used an analysis method termed ‘early-time’ for monitoring the water content in clay-rich soil, and compared the results with time-domain reflectometry (TDR) data. Cheung and Lai (2018) successfully demonstrated the GPR application for leakage detection during a large scale experiment.

There are a number of factors which can limit or eliminate the use of GPR by attenuating its signal reflection, including: the presence of the clayey soil (Rogers *et al.*, 2008), iron oxide produced by a corroded buried cast iron pipe (Van Dam and Schlager, 2000; Pennock *et al.*, 2014), dissolved metallic ions (Deceuster and Kaufmann, 2005), depth of the water table (Bano, 2006). Pennock *et al.* (2010) examined the reduction in GPR reflection that could occur with corroded materials, based on altered soil permittivity and conductivity initiated by corrosion processes and/or products. The Finite Difference Time Domain (FDTD) technique was used to model the scenario of surveying a deteriorated cast iron buried in soil contaminated by corrosion products using the GPR technique. The results showed a substantial reduction in GPR reflection, between 20dB to 30dB, which was identified as significant enough to make a deteriorated iron pipe buried in a 5cm to 10cm zone of contaminated soil undetectable by traditional GPR antennas.

The performance capability of GPR is strongly dependent on the soil electrical conductivity; where in a high soil conductivity attenuation of the radar signal can severely restrict the maximum penetration depth. Graphitic corrosion in cast iron pipes releases iron ions ( $Fe^{2+}$ ) into the surrounding soil, increasing the total dissolved salt content of the soil, and

consequently changing soil conductivity and permittivity (DeBerry *et al.*, 1982; Moghareh Abed *et al.*, 2013; Moghareh Abed, 2016). As for the GPR these electromagnetic parameters are linked with the velocity (m/s) and the attenuation coefficient (Np/m) of the signal. For this reason, fundamental electromagnetic parameters for example dielectric permittivity, electrical conductivity (EC) and magnetic permeability need to be identified. The electrical conductivity of soils increases with increasing water, soluble salt and/or clay contents (McNeill, 1980). In soils, the most significant conduction-based energy losses are due to the ionic charge transport in the soil solution and electrochemical process associated with cations on clay minerals (Neal, 2004). These losses can seriously impact the performance of GPR (Campbell, 1990; Olhoeft, 2000). Iron oxide in its red rust form is relatively insulating, and it has a relative permittivity that is higher than that of most soils. As the iron pipe is the source of the iron oxide, a higher concentration of the oxide can be expected nearer the pipe. In addition, the corrosion process creates salts at the surface of the pipe, and this produces high conductivity (Pennock *et al.*, 2010). For these reasons, the corroded cast iron pipe can become undetectable with GPR.

Even though much research has been conducted into GPR applications, there is still a lack of knowledge on the use of GPR for locating and assessing buried utilities in specifically fine-grained soils. Thus, this paper seeks to define GPR boundaries with respect to its ability to assess the condition of cast iron pipes in fine-grained soils, understanding the problem of poor detection of cast iron pipes in fine-grained soils.

### **3 Methods**

This section describes the laboratory-based testing methodology devised to meet the aim of this research, i.e. to help understand how the released ions from corroding cast iron influence changes to the soil properties, particularly those affecting GPR, such as electromagnetic properties, and the extent and degree of influence these changes have with time or increasing corrosion. A series of experimental testing arrangements were designed to help understand the complex interactions occurring when buried cast iron pipes corrode within soils. Furthermore, the FDTD method was utilised to simulate GPR signals investigating impacts of a corroded buried cast iron pipe on the GPR signal by considering the changed conductivity.

### 3.1 Arrangement of the Laboratory Experiments

Since corrosion of a pipe buried in soil naturally occurs slowly, the reaction was accelerated in the laboratory experiments by inducing an electrical potential across the test samples, using the principles of electro-osmosis and electromigration (electrokinetics) (Clarke *et al.*, 1990; Schmidt, 2007). This method was selected over alternative options so as to avoid introducing any additional ions apart from the ones generated as by-products of the cast iron corrosion (essentially iron ions) so the changes on clay soil properties could be investigated. Furthermore, it would have been difficult to relate the results to the real *in situ* conditions if other ions had been introduced.

This electrokinetic modification induces the migration of  $H^+$  (formed at the anode) and  $OH^-$  (formed at the cathode) towards the oppositely charged electrodes, which generates acid (at the anode) and alkaline (at the cathode) fronts across the test specimens, and hence a pH variability occurs (ranging from acidic pH 2 to alkaline pH 12). These fronts migrate towards each other under the electrical gradient, with the clay being neutral where these fronts meet (Tajudin, 2012). The acid front produced at the anode causes desorption, dissolution and ionisation of cations, migrating towards the cathode.

The experiment was designed to be both practical (i.e. in terms of size and ease of assembly) and accurate (less than 5% variation in results). It was found impractical to design small scale experimental processes within the laboratory that could support a GPR survey. Therefore, the primary focus of the experimental study was shifted to evaluating the conductivity and permittivity, i.e. the electromagnetic properties, of the clay soils via TDR, as well as the physico-chemical characterisation of the test specimens. The TDR results were used as a surrogate for the likely performance of GPR due to underlying principles being analogous (Curioni *et al.*, 2017).

Two types of clay were investigated during the experiment, a relatively inactive Kaolin Clay and Oxford Clay, which is more active and has mixed mineralogy, as described in Table 1. These two clay types were chosen to provide a platform for comparison of behaviour, due to their different natures (predominantly single and mixed mineralogy) and properties. Following the lead of many researchers working in the field of electrokinetics (e.g. Barker *et al.*, 2004; Liaki, 2006), it was decided to use a relatively pure form of kaolinite (termed herein Kaolin Clay). However, for translation of the results to practice, while retaining the ability to compare results with previous researchers and therefore aid in extrapolating the results (e.g. Barker *et*



*al.*, 2004; Schmidt, 2007), a clay of mixed mineralogy (Oxford Clay, which is illite-rich) was chosen to act as a comparator.

Consolidation, rather than compaction, was chosen as the means of soil sample preparation in order to avoid the possible creation of air voids and non-uniformity across the sample, both of which could adversely affect the results (Terzaghi *et al.*, 1996; Venkatramaiah, 2000).

A simple schematic of the experimental arrangement adopted for the testing is shown in Figure 2. A cast iron disc was used in the accelerated corrosion tests that had similar properties and composition to old cast iron pipelines, in order to help relate the test results to field conditions. Utilisation of the disc rather than a real cast iron pipe section was due to the difficulties of producing consolidated samples in contact with cast iron pipes, and also trying to keep the scale of the experiments to a workable size. The other difference with the field condition was the absence of phosphorous in the composition of the disc, due to health and safety considerations (i.e. potential kidney damage) (Sim *et al.*, 2013). A cathode was created from a graphite-coated electrode (or Electrokinetic Geosynthetic, EKG; the coating prevented corrosion of the electrodes and hence any ions being released from the electrodes) (Figure 2). The experimental cell consisted of a Perspex cylinder for consolidating the clay samples, with dimensions of 210 mm height and 102 mm internal diameter. Part 1 in Figure 2 consists of PVC plates placed on top of the specimen for transferring the consolidation load, with holes were provided for water inlet and outlet. In addition, a filter paper (a glass microfiber Whatman 0.20  $\mu\text{m}$  membrane filter) was placed between the PVC plates and the cast iron disc to facilitate to two-way consolidation drainage. Part 2 consisted of a 10 mm thick cast iron disc (the source of corrosion – anode), and wires attached to its upper surface, placed below the filter paper. Part 3 was the experimental cell containing the consolidated soil specimens, which was attached to Part 4, the bottom PVC plate, which housed the cathode and had a single water outlet.

Control tests were conducted in which no cast iron disc were used. The control tests were constructed in the same way as described above, the only difference being that the cast iron disc was replaced by EKG to form the anode. The time periods for the experimental tests using the cast iron discs were 2, and 4 weeks, and 3 months, while tests without the cast iron disc lasted for 2 and 4 weeks for both Kaolin and Oxford clay soils.

The samples were kept hydrated over the period of current injection by maintaining a water feed with a nominal pressure head at the anode to compensate for cathodic draining due to the

electrokinetic processes. This helped to prevent the sample drying out and any potential thermal flux forming at the anode.

### **3.2 Geochemical Properties Monitoring**

The geochemical assessments were essential to determine component release, and assess how the surrounding soils were chemically modified due to the cast iron corrosion. To evaluate the solubility properties of the iron oxyhydroxides, and the amount of iron that could be absorbed by the clay in addition to the precipitated salts, an ion leaching assessment and compositional analysis [X-ray fluorescence (XRF) method] were carried out, and these were validated by a pH modification assessment. pH Dependence Leaching Test, CEN/TS 14429 (CEN, 2008), determines the pH-dependency of ion solubility, complexation or precipitation which was conducted along with Iron Solubility Assessment, ASTM D4646-03 (ASTM, 2008), to understand the behaviour of iron solubility during the release of iron ions from the buried cast iron pipes.

From the corrosion of cast iron, the released iron ions readily form iron oxyhydroxides and are theoretically expected to have low solubility, which therefore mandates an evaluation of the solubility conditions within the experimental clays, as well as the maximum amount of iron ions that can be absorbed or complexed by the clay, in addition to co-precipitation of ions (Schwertmann, 1991). To evaluate the solubility properties of iron oxyhydroxides and the amount of iron ions that could be removed from the soluble fraction by the clay soils in addition to insoluble or precipitated salts, iron solubility tests were adapted and undertaken.

The electrokinetic method induces a variable pH modification within the soil, due to ion migration between the anode and cathode. This necessitates an understanding of the solubility and precipitation behaviour of the released ions (of interest) within the pH domain (pH 2-12 expected from the anode to the cathode). Therefore, a pH-dependent solubility evaluation was essential to assess the maximum soluble availability of the ions of interest (iron), as well as the solubility behaviour across the pH range.

The electrical conductivity (EC) of a solution is the measure of its ability to conduct electricity and serves as an estimate of the total amount of dissolved salt or of dissolved ions. EC measurements were conducted in a temperature-controlled room ( $21\pm1^{\circ}\text{C}$ ) as the solubility level is sensitive to temperature. A Hanna Hi 9033 multi-range meter was employed for elute

measurements during testing and the test was carried out in accordance with BS 1377-2 (BSI, 1990). EC was also measured using the TDR method, as described in Section 3.4.

### **3.3 Physical/Geotechnical Properties Monitoring**

To fully understand a chemically modified soil, it is important to evaluate the physical changes in the soil properties. The physical changes measured included moisture content, undrained shear strength (USS) and Atterberg limits. Atterberg limit tests are feasible for small sample volumes using methods based on the Casagrande method in BS 1377-2 (BSI, 1990). The USS was measured using the fall cone test (Hansbo, 1957; Moghareh Abed, 2016) and allowed differential changes in shear strength to be observed within the sample induced by the electrochemical treatment and the migration of ions. The USS of clay depends on factors such as cation exchange, salt precipitation and clay mineral dissolution and cementitious product formation and crystallisation, which cause changes in structure and mineralogy. The moisture content was measured before the consolidation process (to check the initial moisture content of the sample) and after the electrokinetic process.

### **3.4 Geophysical Properties Monitoring**

Changes in geophysical properties, including permittivity and conductivity, of the soil were monitored using the TDR method. The method involves an electrical wave being transmitted through metal rods of a waveguide into the soil and then being reflected back to the generator (Rhoades *et al.*, 1976; Annan, 1977). From an analysis of the travel time or signal propagation velocity ( $V_p$ , a function of the cable dielectric constant), it is possible to determine the bulk electrical conductivity of the soil (Castiglione *et al.*, 2006; Curioni, 2013). The ions in the soil provide a path for electrical conduction between the TDR and probe rods (Jones *et al.*, 2002). TDR readings were taken using a TDR100 cable tester and CS645 (with 75mm long probes) supplied by Campbell Scientific Ltd (2019).

### **3.5 GPRMax 2D/3D Modelling**

GPR modelling was used to demonstrate the practical effect of the experimental results in a simulated scenario. Using the permittivity and conductivity data obtained from the TDR measurements obtained from the test samples at different times, simulations were performed using the GPRMax software (Giannopoulos, 2005). The GPRMax software uses the Finite Difference Time Domain (FDTD) method for modelling GPR, where all electromagnetic

phenomena are described by Maxwell's equations. In addition, the compositional, geotechnical and geochemical characterisation results from the test soils were used to undertake the FDTD simulations. A model was created that simulated a cast iron pipe with a radius of 0.1m buried at a depth of 0.5m and surrounded by homogenous clay (Figure 3). The magnetic permeability was not measured directly for the test soils and assumed to equal 1 in the simulation (Machado *et al.*, 2009). Even though the soil close to the corroding pipe is iron enriched, its magnetic permeability is relatively small compared to the conductivity, and therefore had minimal influence on the simulation outcome. The permittivity and conductivity of the soil in proximity to the cast iron pipe was altered in the simulations to represent changes observed in the experiments. The model simulated a GPR antenna, with a centre frequency of 700MHz (a typical value for this type of GPR survey), moving across the ground surface, with readings taken every 25mm along the transect.

When trying to apply the methodology presented in this paper for field conditions, care needs to be taken as there are many factors that could affect the corrosion process. These factors include the ground water conditions (e.g. the chemical quality of the water in the ground and also the acidity of the rain falling on the ground), the conductivity and pH of the soil, the temperature conditions, the pipe burial depths, the oxygen levels in the ground (aeration), the chemicals in the soil (e.g. contaminants, bacteria or organic content of the soil), the soil corrosivity and its mineralogy and soil porosity.

## **4 Results**

This section describes the laboratory results, including the geochemical, geotechnical and geophysical results. The GPR modelling results are also presented in this section. As the electrokinetic treatment was used to speed up the corrosion process, the results are presented in two groups; the results for tests in which no cast iron disc was used (the control tests), which shows only the effect of the electrokinetics on the Kaolin Clay and Oxford Clay samples, and the results for tests where a cast iron disc was present.

## 336 4.1 Geochemical Results

### 337 4.1.1 Iron Content Concentration

338 It was necessary to determine the amount of iron (as an oxide element) at different locations  
339 within the samples, working from the anode to the cathode, in order to compare the different  
340 behaviour throughout the samples.

341 The concentration of iron in Kaolin Clay samples without a cast iron disc did not change to any  
342 significant extent as no *Fe* was released into the sample from the electrodes (Figure 4). In this  
343 case, the *Fe* behaviour depends on the pH, as the dissolution of the clay minerals is dependent  
344 on the pH environment and the only source of *Fe* is from the clay minerals, and the quantity of  
345 *Fe* in the Kaolin Clay is relatively small. Only small changes were seen around the anode area,  
346 i.e. 1.38% and 1.41% increase for the 2-week and 4-week samples respectively, compared to  
347 the 'natural' value of 1.10% – and these decreased marginally towards the cathode. When the  
348 cast iron disc was used in the tests with the electrokinetic treatment, due to the release of *Fe*  
349 from the anode and its migration within the clay samples, these values increased considerably  
350 to 8.54%, 8.98% and 9.58% for the 2-week, 4-week and 3-month samples at the anode (i.e.  
351 close to the cast iron disc). The iron concentration decreased rapidly away from the anode and  
352 more generally towards the cathode, due to the low solubility of the iron oxyhydroxides  
353 released from the cast iron disc, but the concentrations through the clay profile remained higher  
354 than those without any *Fe* introduced from the cast iron. There was also an increased iron  
355 concentration at the cathode, due to electro-osmotic migration from the iron ions introduced at  
356 the anode, with the concentration at the cathode increasing with time from 2 weeks to 3 months.  
357 Added to this pattern of iron oxyhydroxide migration, dissociation of the Kaolin Clay at the  
358 cathode will also induce the complexation of migrated iron to form stable precipitates towards  
359 the cathode.

360 The 'natural' value of iron concentration in the Oxford Clay was determined as 7.11%. For the  
361 samples that had no cast iron disc (only EKG), the electrokinetic treatment caused an increase  
362 to 7.33% and 7.36% after 2 weeks and 4 weeks respectively, and the amount decreased toward  
363 the cathode, reaching 7.09% and 7.07% (after 2 weeks and 4 weeks respectively) (Figure 8).

364 When a cast iron disc was introduced in the tests with Oxford Clay, the amount of iron  
365 increased to 10.76%, 29.39% and 32.98% for 2 weeks, 4 weeks and 3 months respectively, i.e.  
366 after 3 months the value of the iron oxide concentration increased to 3 times that of the 2-week

sample and nearly 5 times that of the 'natural' measurement. In the 2-weeks sample, i.e. the initial phase of cast iron disc degradation, almost all the introduced Fe complexes and there is minimal movement through the sample as there is enough exchangeable ion in Oxford Clay sample. Thus, the amount of iron in the clay away from the anode (i.e. at 10mm from the anode at 2 weeks and 20mm from the anode at 4 weeks) did not increase until the treatment had been applied for 3 months, where evidence of iron (possibly as precipitation as oxyhydroxides, though the pH will govern whether or not precipitation has occurred) in the middle of the sample was found: it reached a maximum of 18.69% 50mm from the anode and, although reducing towards the cathode, the concentration remained elevated at all points until the cathode is reached.

#### 4.1.2 pH

The pH of both soils was changed by electrokinetic treatment such that it ranged from approximately 3 to 12 (see Figure 5). Both soils had the same behaviour in relation to the test without a cast iron disc. However, when a cast iron disc was involved in the test, there was a 'jump' in the pH trend for Kaolin Clay samples at 2-weeks, 4-weeks and 3-months (e.g. this 'jump' occurred midway along the sample (50-60mm away from the anode) from a baseline of approximately 3.5-4.5 at 3-months in Figure 5); this trend was attributed to the meeting of acid and alkaline fronts where migrated  $H^+$  and other cations from the anode interact with  $OH$  ions migrating away from the cathode.

The 3-month sample of Oxford Clay was more acidic at the anode, due both to the high Fe release from the cast iron disc and also due to the increased potency of the hydrolysis reactions releasing  $H^+$  ions with time of treatment (see Figure 5). The pH curve for the Oxford Clay sample, in contrast to the Kaolin Clay, showed a clear uniformly-rising trend with increasing distance from the cast iron disc. At 50mm away from the cast iron disc, the pH of the Kaolin Clay drops to 3.53 (i.e. becomes more acidic) at an iron concentration of 4.06% (which increased from 1.80% to 4.06% between 4 weeks and 3 months). However, at 70mm away from the disc, the amount of Fe concentration increased to 4.59% which is associated with a significant incremental change in pH to 8.67. Developing highly acid and alkaline environments at the anode and cathode, respectively, equated with a significant increase in USS (see Figure 6).

Figure 6 presents the relationship between the USS and water content for the treated Kaolin Clay samples with and without a cast iron disc. The data above the control line (in red) shows

soil strengthening, i.e. due to chemical reactions, in accordance with ideas presented by Rogers *et al.* (2003) and Liaki *et al.* (2008). This is mainly due to mineral dissolution, and subsequent crystallisation. Therefore, it can be proposed that the arrows in the figure (left corner side of the figure) show soil weakening (i.e. chemical deterioration). In Figure 6, the circled points denote the data points adjacent to the anode, while the squared points represent data points close to the cathode. The general observation is that all the points close to the cathode are markedly weaker than the anode points when a cast iron disc was used. A lower pH at the anode and a higher pH at the cathode at 4 weeks shows some strengthening from the low points at 2 weeks, with the data at the cathode being significantly closer to the control line. The cast iron disc (the source of iron ions) and the more extreme range of pH evidently cause the undrained shear strength to increase. As for the 2-weeks and 4-weeks samples the stronger acid ( $\text{pH} < 3$ ) and base ( $\text{pH} > 11.6$ ) environments have developed and the shear strength has increased considerably. The increased iron content near the anode caused the greatest increase in undrained shear strength, for the reasons stated above, while the described reactions near the cathode account for the more modest strength increases in this region. These chemical effects are shown to be evidently greater for the 3-month sample, i.e. the data points exist farther above the control line.

#### 4.1.3 Conductivity

Figure 7 presents the results of the conductivity measurements for the Kaolin Clay and Oxford Clay for the 3-month sample with a cast iron disc. The first major difference between these two types of clay is that the Oxford Clay has higher conductivity due to its more mixed mineralogy (hence soluble ion content). Both graphs show a similar trend, i.e. a high conductivity at the anode, which was attributed to high  $H^+$  and  $Fe$  concentrations, and also due to the solubility of ions at low pH in the case of Oxford Clay. Figure 7 also shows high conductivity at the cathode for the Kaolin Clay, which was attributed to ion solubility at high pH in a clay that is relatively stable at low pH. The conductivity of Oxford Clay follows a similar trend to the iron concentration. It is therefore evident that the amount of iron released through the clay soil has a direct relationship with soil conductivity. This trend is also evident in Figure 7 for the Kaolin Clay sample with the exception of the measurements at the cathode, where the  $Fe$  concentration remains relatively low (hence the attribution of the raised conductivity to clay mineral dissolution, stated above). However, the conductivity for Oxford Clay did not follow the same trend as that for Kaolin Clay, which can be attributed to three reasons: the extent of  $Fe$

migration, the precipitation of ions complexing with cations (a factor related to inherent solubility), and cementation and crystallisation at the cathode.

## **4.2 Geotechnical Results**

### **4.2.1 Undrained Shear Strength – Cone Penetration Test**

Figure 8 shows that at 3-months, the Oxford Clay produced a higher USS than the Kaolin Clay, due to both higher concentrations of *Fe* (causing a greater, although similar, pattern of thinning of the diffuse double layer and salt precipitation than in the Kaolin Clay), and also higher availability of other cations to engage in these processes. Figure 8 also shows a marked rise in USS in the lower half of the Oxford Clay sample, this being attributed to the formation of Calcium Silicate Hydrate (CSH), Calcium Aluminate Hydrate (CAH) and/or Hydrated Calcium Aluminosilicate (CASH) gel and crystallisation reactions noting that calcium is available in Oxford Clay but not Kaolin Clay.

In general, the results for the Oxford Clay compared with the Kaolin Clay showed that the Oxford Clay had been more affected by the cast iron corrosion, and in turn accelerated *Fe* release (hence corrosion). Therefore, failure of cast iron pipes is more likely in Oxford Clay than in Kaolin Clay, in spite of the fact that the Kaolin Clay is more acidic. The higher conductivity of the Oxford Clay relative to Kaolin Clay supports this argument, and would suggest that the clay also has higher corrosivity as a result of these features.

### **4.2.2 Moisture Content**

Moisture content was measured before the consolidation process and after the electrokinetic process. The moisture content values were found to lie between approximately 41% and 58% for Kaolin Clay and approximately between 50% and 58% for Oxford Clay both with a cast iron disc. The moisture content of some samples, such as at 3 months, is lower at the bottom of the sample where the cathode was located. This was expected since when iron ions are released through the system, the changes in the diffuse double layer (i.e. thinning of this layer) cause the solid particles to move closer together, and hence the moisture content decreases. In addition, the sample was kept moist at its top end (anode) during the experiment.



#### 4.2.3 Atterberg Limits

The Liquid Limit of the Kaolin Clay and Oxford Clay samples increased generally over time between 2 weeks to 3 months (Figure 9). The increase was attributed to the higher valency (iron) ions coming into the system from corrosion of the cast iron disc (the anode). Another reason was the thinning of the diffuse double layer via cation exchange as the treatment period became longer (although the iron ion concentrations increased only marginally, along with a marked increase in conductivity at the anode that was attributed to a fall in pH at the anode to values significantly below 4.0). Conversely in the alkali environment at the cathode ( $\text{pH} > 11.5$ ), the opposite phenomenon occurs where the diffuse double layer thickness increases and, combined with conditions in which salt precipitation is encouraged, therefore a reduction in Liquid Limit was observed.

Figure 9 illustrates that after an initial rise from the 'natural' value of 23.6%, the Plastic Limits generally decreased over time for Kaolin Clay between 2 weeks and 3 months, although the data for the 2-week and 4-week tests were approximately similar throughout the sample and it was only after 3 months that a significant fall occurred. Bohn *et al.* (2002) stated that a low pH ( $\text{pH} < 4.7$ ) in general caused multivalent cations of Al, Fe and Mg to be released from degradation of the clay minerals into the pore fluid. These multivalent cations are strongly attracted by the negatively charged clay surface and contribute to thinning of the diffuse double layer, hence raising of the Plastic Limit.

The main contributory factors to the increasing shear strength values (the accumulation of precipitates and modification of the mineralogy via cation exchange) as a result of the electrochemical reactions, are thus reflected in the results of the Liquid Limit tests, and are linked to the pH gradient and Fe concentration.

Based on the results presented it was found that the Kaolin Clay soil was less aggressive than the Oxford Clay soil, i.e. the corrosion activity was stronger in the Oxford Clay, and this led to cementation, precipitation and complexation. At the end of the tests the cast iron discs were examined, and this difference in corrosion activity could clearly be seen. An example of the cast iron discs for the 3-months samples are shown in Figure 10, with the disc in the Oxford Clay showing a much more uneven and pitted surface compared to the disc in the Kaolin Clay. Essentially the Oxford Clay presented a much more aggressive environment due to its mixed mineralogy (including the more active smectite clay mineral) and the different ions released and migrating through the soil.

### 4.3 *GPRMax 2D/3D Modelling Results*

FDTD simulations were used to simulate GPR signals to investigate buried cast iron pipes in clay soil in relation to the measured soil conductivity, permittivity and other factors influencing clay modification induced by cast iron pipe corrosion (the values used as input to the simulation which were measured during the experiment are listed in Table 2). The simulation was based on the model shown in Figure 3.

The results from the simulation of a cast iron pipe buried in Kaolin Clay showed that the pipe could be clearly observed by the GPR for all the values input from the laboratory tests at the different time intervals (Figure 11). This meant that the properties of the soil had not been modified in a way that prevented the pipe from being detected by a GPR unit with a 700MHz antenna at 0.5m depth.

The simulations for Oxford Clay showed different results. Although the results using the input values from the 4-weeks sample showed that the characteristics of the pipe were clearly detected by the GPR (Figure 12a), the results for the 3-months sample (Figure 12b) showed that the GPR was unable to detect the pipe. This was attributed to the Oxford Clay modification due to the corrosion process. Since the major difference between the Kaolin Clay and the Oxford Clay reactions to accelerated cast iron corrosion concerned the stabilisation reactions involving CAH, CSH and/or CASH, as noted previously, then this aspect of ground modification in relation to GPR applications is worthy of further investigation, although other features (such as the markedly raised *Fe* concentrations away from the cast iron pipe) might also have an influence.

Additional simulations were conducted using interpolated and extrapolated input values. For example, to see at what approximate time (in relation to the laboratory test results) the pipe became undetectable in the Oxford Clay, which was determined as about 9-weeks (Figure 13). For the simulation involving the pipe buried in Kaolin Clay, the laboratory values were extrapolated to 60-weeks and input into the simulation, and the pipe still remained visible by the GPR.

These are obviously relatively simple simulations using values obtained from small scale laboratory tests. However, these do illustrate the potential effect of changing soil parameters locally to a cast iron pipe could limit GPR surveys from locating corroded cast iron pipes. Conversely, if GPR surveys are done ‘regularly’ at a particular location, the results could

provide an indication of when there might be considerable corrosion occurring in a cast iron pipe and hence a condition assessment might be warranted.

## **5 Discussion**

Kaolin Clay and Oxford Clay have different mineralogies, therefore their physical and chemical properties change differently during the corrosion process. These changes could be expected to be correlated with the amount of iron concentration, which depends on the amount of iron released from the corrosion and transported through the surrounding clay. There is a high content of iron in Oxford Clay as a relatively active soil compared to Kaolin Clay. The 3-month sample (the longest test) produced the largest values for the migration of Fe and formation (hence concentration) of iron oxyhydroxides in the soil. Also, due to the precipitation of iron hydroxide close to cathode side and extending into the body of the sample of Kaolin Clay the amount of iron was increased for both types of soils, yet in different patterns. These reactions were affected by the soil's pH, as the dissolution of clay minerals is dependent on the pH environment.

The pH of both soils was changed such that it ranged from approximately 3 to 12 by electrokinetic treatment. Developing highly acid and alkaline environments at the anode and cathode, respectively, equated with a significant increase in USS and was accompanied by the ions presence in the soil system. This corresponds to the idea that the corrosion was due to an electrochemical process, which converted metal substrates to oxides, hydroxides and aqueous salts within the cathode-anode system (Pritchard *et al.*, 2013). Also, the rate of corrosion increased with increases in the electrical conductivity of soil, as reported by Ekine and Emujakporue (2010).

The results for conductivity measurements of Kaolin Clay and Oxford Clay for the 3-month sample with a cast iron disc, show a major difference between these two types of clay as the Oxford Clay has relatively high conductivity due to its more mixed mineralogy (hence soluble ion content). The conductivity of Oxford Clay follows a similar trend to its iron concentration. It is therefore evident that the amount of iron released through the clay soil has direct relationship with soil conductivity. However, the conductivity for Oxford Clay did not follow the same trend as that for Kaolin Clay, which can be attributed to three reasons: extent of Fe

551 migration, precipitation of ions complexing with cations (a factor related to inherent solubility),  
552 and cementation and crystallisation at the cathode.

553 The USS of Oxford Clay was higher than that for Kaolin Clay, due to both higher  
554 concentrations of Fe (causing a greater, though similar, pattern of thinning of the diffuse double  
555 layer and salt precipitation than in the Kaolin Clay), but also higher availability of other cations  
556 to engage in these processes.

557 The findings of this study are in contrast with part of the conclusion drawn by Pennock *et al.*  
558 (2010), who suggested that for clayey soil in general only “old” corroded iron pipes that  
559 contaminated the surrounding soil can become undetectable. While, the current study show that  
560 it depends on the type of clay, as in Oxford Clay the process of becoming undetectable can be  
561 quite fast, if the required condition was provided. However, the findings of this study confirms  
562 the observations made by von Wolzogen Kühn and Van der Vlugt (1964), where accelerated  
563 corrosions of cast iron pipes in some specific clay was reported in the field, and the laboratory  
564 experiments on London Clay by Schmidt *et al.* (2006). It has been noted that buried corroded  
565 cast iron pipes tend to be less visible to Ground Penetrating Radar (GPR) locating methods  
566 than non-corroded pipes, which has implications for detecting these utilities and safe working.  
567 Some of the results from this research, in terms of the likely electrical properties of the soil  
568 surrounding a corroded cast iron pipe, contributed to research aimed at helping understand the  
569 frequencies required for GPR to maximise the chances of detecting such pipes, and this work  
570 was reported in Pennock *et al.* (2014). The study by Pennock *et al.* (2014) revealed that the  
571 frequency of the GPR antenna is an influential factor in detecting corroded iron pipes when  
572 using the GPR method. The results of a series of numerical analyses showed that a corroded  
573 iron pipe buried in clay soil would be still detectable at frequencies less than or equal to 100  
574 MHz, but at higher frequencies the pipe visibility decreases markedly.

575 As a result, the experimental results presented in the current paper can enhance the decision  
576 making process when locating or assessing iron pipes using the GPR method by providing  
577 information on the likely electrical properties of the soil surrounding the pipe and hence the  
578 choice of GPR to be used. This information could decrease the number of hazardous and costly  
579 utility strikes as the use of unsuitable geophysical methods has been identified as one of the  
580 main causes of utility strikes (Makana *et al.*, 2018).

## 581    **6    Conclusions**

582    The corrosion of cast iron pipes buried directly in clay soils is one of the major challenges to  
583    the water industry in managing an ageing water distribution network in countries where cast  
584    iron features predominantly in the buried infrastructure. The corrosion occurs in the saturated  
585    zone of clay soil by electrochemical oxidation of the cast iron in contact with oxygenated water.  
586    The development of the corrosion process results in a galvanic cell being set up between the  
587    pipe (the anode) and the clay (a distributed cathode) and the pH change in this system causes  
588    iron ions to be released and corrosion products, such as iron oxide, iron hydroxide and aqueous  
589    salts, to form in the surrounding clay soil. Excavation to locate buried cast iron pipes, assess  
590    their condition and monitor their degradation is both disruptive and expensive and hence  
591    remote surveying using geophysical techniques, notably GPR, has been proposed to address  
592    this. It is important, therefore, to understand the influences of cast iron degradation on clay  
593    soils and their implications for GPR surveying.

594    The aim of this research was to gain a better understanding of how the ions released from cast  
595    iron corrosion in clay soils, i.e. Oxford Clay and Kaolin Clay, change the soil properties, and  
596    how the extent and degree of this influence changes with time, and additionally to investigate  
597    the effect of these changes on the efficacy of GPR surveying.

598    The results for the Oxford Clay, compared with the Kaolin Clay showed, that it had been more  
599    affected by cast iron corrosion, and in turn causes enhanced Fe release (hence corrosion).  
600    Therefore, failure of cast iron pipes would be expected to be more likely in Oxford Clay than  
601    in Kaolin Clay, in spite of the fact that the Kaolin Clay is more acidic, and this lead to  
602    cementation as well as the cation exchange, complexation and precipitation reactions. The  
603    higher conductivity of the Oxford Clay relative to Kaolin Clay supports this argument, and  
604    would suggest that the clay also has higher corrosivity as a result of these features.

605    The FDTD simulation result showed that the properties of the Kaolin Clay, and for different  
606    time periods, had not been modified in a way that prevented the pipe from being detected by  
607    the GPR with a 700MHz antenna. The simulations for Oxford Clay showed different  
608    behaviours, as GPR was unable to detect the pipe after approximately 7-8 weeks, and this was  
609    attributed to Oxford Clay modification due to the corrosion process. Further simulation  
610    indicated that for a saturated clay soil such as Kaolin Clay, GPR signals are not significantly  
611    attenuated and therefore the pipe can be detected while corrosion of the cast iron pipe advances.

Some of the key observations from the tests are as follows:

- Iron ions (Fe) is released as a product of cast iron corrosion, causing the clay soil close to the cast iron (disc) to create a low pH (acidic) condition, lower than when no cast iron disc was used, and this lowered pH developed progressively with time.
- In Oxford Clay, due to its mixed mineralogy, the low pH conditions, makes Oxford Clay relatively unstable, where evidence suggests dissolution of Oxford Clay minerals, as the Fe and other cations migrated towards the cathode and substituted on the cation exchange sites of the clay
- USS measurements for Kaolin Clay, showed raised strength for all three periods when simulating cast iron corrosion, which was attributed to chemical modification in the clay. However, in Oxford Clay the increased strength was evident in the lower half of the samples, and especially at the cathode, due to the stabilisation reactions.

Based on the findings of this study Oxford Clay should be avoided around a cast iron pipe as it has the potential to cause aggressive corrosion and failure in a relatively short period. The parameters which can be considered in assessing the condition are:

- Geochemical properties; to evaluate the solubility properties of the iron oxyhydroxides, utilising pH Dependence Leaching Test, and Iron Solubility Assessment
- Physical/Geotechnical properties; to understand the physical changes in the soil properties including moisture content, undrained shear strength (USS) and Atterberg limits and cone penetrometer test
- Geophysical properties; to monitor changes in permittivity and conductivity, using the TDR method.

Recommendations for further study are provided below:

- Repeating tests for different types of soil, to gain a more extensive dataset
- Conducting additional chemical analysis, to understand the behaviour of iron solubility conditions of the iron oxyhydroxides and the maximum amount of iron that could be absorbed
- Validating the laboratory findings with field experiments; utilising cone penetrometer test as a comparative test for USS in very small samples is also be considered
- Determining the effect of cast iron corrosion using other methods rather than the electrokinetic system.

## 7 Data Availability

Some or all data, models, or code that support the findings of this study are available from the corresponding author upon reasonable request.

## 8 Acknowledgement

The authors acknowledge the support provided by the Engineering and Physical Sciences Research Council (EPSRC) for the project grants Mapping The Underworld (EP/F065965), Assessing The Underworld (EP/K021699) and Balancing the Impact of City Infrastructure Engineering on Natural Systems using Robots (EP/N010523/1).

## 9 References

- Algeo, J., R.L. Van Dam and L. Slater (2016). "Early-Time GPR: A Method to Monitor Spatial Variations in Soil Water Content during Irrigation in Clay Soils." Vadose Zone Journal **15**(11).
- Annan, A.P. (1977). "Time-domain reflectometry-Air-gap problem in a coaxial line, report of activities, part B." Papers from the Geological Survey of Canada **77-1B**: 55-58.
- ASTM (2008). Standard test method for 24-h batch-type measurement of contaminant sorption by soils and sediments, ASTM D-4646-03. American Society of Testing Materials West Conshohocken, PA.
- Atef, A. (2010). Optimal condition assessment policies for water and sewer infrastructure. M.Sc. Thesis, Nile University.
- Ayala-Cabrera, D., M. Herrera, I. Montalvo and R. Pérez-García (2011). "Towards the visualization of water supply system components with GPR images." Mathematical and Computer Modelling **54**(7-8): 1818-1822.
- Bach, P.M. and J.K. Kodikara (2017). "Reliability of Infrared Thermography in Detecting Leaks in Buried Water Reticulation Pipes." IEEE Journal of Selected Topics in Applied Earth Observations and Remote Sensing **10**(9): 4210-4224.
- Bano, M. (2006). "Effects of the transition zone above a water table on the reflection of GPR waves." Geophysical research letters **33**(13).
- Barker, J.E., C.D.F. Rogers, D.I. Boardman and J. Peterson (2004). "Electrokinetic stabilisation: an overview and case study." Proceedings of the Institution of Civil Engineers- Ground Improvement **8**(2): 47-58.
- Belver, C., M.A. Bañares and M.A. Vicente (2002). Preparation of Porous Silica by Acid Activation of Metakaolins. Studies in Surface Science and Catalysis. F. Rodriguez-Reinoso, B. McEnaney, J. Rouquerol and K. Unger, Elsevier. **144**: 307-314.
- Bohn, H.L., R.A. Myer and G.A. O'Connor (2002). Soil Chemistry. New York, Wiley.
- Bonds, R.W., L.M. Barnard, A.M. Horton and G.L. Oliver (2005). "Corrosion and corrosion control of iron pipe: 75 years of research." Journal- American Water Works Association **97**(6): 88-98.
- Bradford, S. (2000). Practical Handbook of Corrosion Control in Soils: Pipelines, Tanks, Casings, Cables. CASTI Publishing Inc, 10566-114 Street, Edmonton, Alberta, T 5 H 3 J 7, 2000. Illustrated.

BSI (1990). BS 1377-2: 1990, Methods of test for soils for civil engineering purposes-Part 2: Classification tests. London: UK: British Standard Institution.

Campbell, J.E. (1990). "Dielectric properties and influence of conductivity in soils at one to fifty megahertz." Soil Science Society of America Journal **54**(2): 332-341.

Campbell Scientific Ltd. (2019). "TDR100 Time-Domain Reflectometer." Retrieved 31/05/2019, from <https://www.campbellsci.co.uk/tdr100>.

Castiglione, P., P. Shouse and J. Wraith (2006). "Multiplexer-induced interference on TDR measurements of electrical conductivity." Soil Science Society of America Journal **70**(5): 1453-1458.

CEN (2008). The pH Dependent Leaching Test with Initial Acid or Base Addition CEN/TS 14429. Brussels, European Committee for Standardisation CEN.

Cheung, B.W. and W.W. Lai (2018). Field Validation of Water Pipe Leak by Spatial and Time-lapsed Measurement of GPR Wave Velocity. 2018 17th International Conference on Ground Penetrating Radar (GPR).

Choi, J., J. Shin, C. Song, S. Han and D.I. Park (2017). "Leak Detection and Location of Water Pipes Using Vibration Sensors and Modified ML Prefilter." Sensors **17**(9): 2104.

Clarke, P., A. Ray and C. Hogarth (1990). "Electromigration—a tutorial introduction." International Journal of Electronics Theoretical and Experimental **69**(3): 333-338.

Cole, I.S. and D. Marney (2012). "The science of pipe corrosion: A review of the literature on the corrosion of ferrous metals in soils." Corrosion Science **56**: 5-16.

Costello, S.B., D.N. Chapman, C.D.F. Rogers and N. Metje (2007). "Underground asset location and condition assessment technologies." Tunnelling and Underground Space Technology **22**(5–6): 524-542.

Curioni, G. (2013). Investigating the seasonal variability of electromagnetic soil properties using field monitoring data from Time-Domain Reflectometry probes. PhD, University of Birmingham.

Curioni, G., D.N. Chapman and N. Metje (2017). "Seasonal variations measured by TDR and GPR on an anthropogenic sandy soil and the implications for utility detection." Journal of Applied Geophysics **141**: 34-46.

DeBerry, D.W., J.R. Kidwell, D.A. Malish, U.S.E.P.A.O.o.D. Water and S. Corporation (1982). Final Report: Corrosion in Potable Water Systems, U.S. Environmental Protection Agency, Office of Drinking Water.

Deceuster, J. and O. Kaufmann (2005). GPR Mapping of a Dissolved Metals Plume Inside an Old Dyeing Plant at Leuze-Belgium. Near Surface 2005-11th European Meeting of Environmental and Engineering Geophysics.

Demirci, S., E. Yigit, I.H. Eskidemir and C. Ozdemir (2012). "Ground penetrating radar imaging of water leaks from buried pipes based on back-projection method." NDT & E International **47**(Supplement C): 35-42.

Demma, A., P. Cawley, M. Lowe, A.G. Roosenbrand and B. Pavlakovic (2004). "The reflection of guided waves from notches in pipes: a guide for interpreting corrosion measurements." NDT & E International **37**(3): 167-180.

Ekine, A. and G. Emujakporue (2010). "Investigation of corrosion of buried oil pipeline by the electrical geophysical methods." Journal of Applied Sciences and Environmental Management **14**(1): 63 - 65.

Fedorova, L.L., D.V. Savvin, M.P. Fedorov and A.S. Struchkov (2016). GPR monitoring of cryogenic processes in subgrade soils. 2016 16th International Conference on Ground Penetrating Radar (GPR), Hong Kong, IEEE.

Folkman, S. (2018). Water main break rates in the USA and Canada: A comprehensive study. Mechanical and Aerospace Engineering Faculty Publications. Paper 174. Logan, UT: Utah State University.



Freeman, S.R. (1999). "Graphitic corrosion-Dont forget about buried cast iron pipes." Materials performance **38**(8): 68-69.

Gagg, C.R. and P.R. Lewis (2011). "The rise and fall of cast iron in Victorian structures—A case study review." Engineering Failure Analysis **18**(8): 1963-1980.

Giannopoulos, A. (2005). "Modelling ground penetrating radar by GprMax." Construction and building materials **19**(10): 755-762.

Hansbo, S. (1957). New approach to the determination of the shear strength of clay by the fall-cone test, Royal Swedish Geotechnical Institute Proceedings No 14.

Hao, T., C.D.F. Rogers, N. Metje, D.N. Chapman, J.M. Muggleton, K.Y. Foo, P. Wang, S.R. Pennock, P.R. Atkins and S.G. Swinger (2012). "Condition assessment of the buried utility service infrastructure." Tunnelling and Underground Space Technology **28**: 331-344.

Liaki, C. (2006). Physicochemical Study of Electrokinetically Treated Clay Soils using Carbon and Steel Electrodes. PhD, University of Birmingham.

Liaki, C., C.D. Rogers and D.I. Boardman (2008). "Physicochemical effects on uncontaminated kaolinite due to electrokinetic treatment using inert electrodes." Journal of Environmental Science and Health Part A **43**(8): 810-822.

Liu, Z. and Y. Kleiner (2013). "State of the art review of inspection technologies for condition assessment of water pipes." Measurement **46**(1): 1-15.

Liu, Z., Y. Kleiner, B. Rajani, L. Wang and W. Condit (2012). Condition assessment technologies for water transmission and distribution systems. Washington DC, USA. **108**.

Machado, V.M., M. Almeida and M.G.d. Neves (2009). "Accurate magnetic field evaluation due to underground power cables." European Transactions on Electrical Power **19**(8): 1153-1160.

Makana, L.O., N. Metje, I. Jefferson, M. Sackey and C.D. Rogers (2018). "Cost estimation of utility strikes: towards proactive management of street works." Infrastructure Asset Management: 1-13.

Makar, J. and S. McDonald (2007). "Mechanical behavior of spun-cast gray iron pipe." Journal of materials in civil engineering **19**(10): 826-833.

Marshall, P. (2001). The residual structural properties of cast iron pipes: structural and design criteria for linings for water mains. 01/WM/02/14. London, UKWIR.

McNeill, J. (1980). Electrical conductivity of soils and rocks, Geonics Limited.

Merdinger, C.J. (1955). "Water Supply through the Ages: Part II Modern Developments." The Military Engineer **47**(319): 359-364.

Metje, N., P.R. Atkins, M.J. Brennan, D.N. Chapman, H.M. Lim, J. Machell, J.M. Muggleton, S. Pennock, J. Ratcliffe, M. Redfern, C.D.F. Rogers, A.J. Saul, Q. Shan, S. Swinger and A.M. Thomas (2007). "Mapping the Underworld – State-of-the-art review." Tunnelling and Underground Space Technology **22**(5–6): 568-586.

Moghareh Abed, T. (2016). Experimental investigation of cast iron corrosion on clay soil and GPR performance. PhD Thesis, University of Birmingham, UK.

Moghareh Abed, T., D.N. Chapman, C.D.F. Rogers and U.E. John (2013). Alteration of soil support to cast iron pipelines due to corrosion. Pipelines 2013: Pipelines and Trenchless Construction and Renewals - A Global Perspective, Fort Worth, Texas, ASCE.

Mooney, J., J. Ciampa, G. Young, A. Kressner and J. Carbonara (2010). GPR mapping to avoid utility conflicts prior to construction of the M-29 transmission line. IEEE PES T&D 2010, IEEE: 1-8.

Neal, A. (2004). "Ground-penetrating radar and its use in sedimentology: principles, problems and progress." Earth-science reviews **66**(3-4): 261-330.

Olhoeft, G.R. (2000). "Maximizing the information return from ground penetrating radar." Journal of Applied Geophysics **43**(2-4): 175-187.

781 Pennock, S.R., T.M. Abed, G. Curioni, D.N. Chapman, U.E. John and C.H.J. Jenks (2014).  
 782 Investigation of soil contamination by iron pipe corrosion and its influence on GPR detection.  
 783 Proceedings of the 15th International Conference on Ground Penetrating Radar.  
 784 Pennock, S.R., D.N. Chapman, C.D.F. Rogers, A.C.D. Royal, A. Naji and M.A. Redfern  
 785 (2010). Effects of iron pipe corrosion on GPR detection. Proceedings of the XIII International  
 786 Conference on Ground Penetrating Radar, IEEE.  
 787 Pritchard, O., S.H. Hallett and T.S. Farewell (2013). Soil corrosivity in the UK–Impacts on  
 788 Critical Infrastructure. ITRC–Infrastructure Transition Research Consortium. Soil Resources  
 789 Institute NSRI, Cranfield University, UK.  
 790 Rainer, A., T.F. Capell, N. Clay-Michael, M. Demetriou, T.S. Evans, D. Jesson, M. Mulheron,  
 791 L. Scudder and P. Smith (2017). "What does NDE need to achieve for cast iron pipe networks?"  
 792 Infrastructure Asset Management **42**(2): 68-82.  
 793 Rajani, B., C. Zhan and S. Kuraoka (1996). "Pipe soil interaction analysis of jointed water  
 794 mains." Canadian Geotechnical Journal **33**(3): 393-404.  
 795 Rhoades, J., P. Raats and R. Prather (1976). "Effects of liquid-phase electrical conductivity,  
 796 water content, and surface conductivity on bulk soil electrical conductivity 1." Soil Science  
 797 Society of America Journal **40**(5): 651-655.  
 798 Roberge, P.R. (2007). Corrosion inspection and monitoring. Hoboken, NJ, USA, John Wiley  
 799 & Sons.  
 800 Rogers, C., C. Liaki and D. Boardman (2003). Advances in the engineering of lime stabilised  
 801 clay soils. International conference on problematic soils, Nottingham, UK.  
 802 Rogers, C.D.F., T. Hao, S.B. Costello, M.P.N. Burrow, N. Metje, D.N. Chapman, J. Parker,  
 803 R.J. Armitage, J.H. Anspach and J.M. Muggleton (2012). "Condition assessment of the surface  
 804 and buried infrastructure–A proposal for integration." Tunnelling and Underground Space  
 805 Technology **28**: 202-211.  
 806 Rogers, C.D.F., N. Zembillas, N. Metje, D.N. Chapman and A.M. Thomas (2008). Extending  
 807 GPR Utility Location Performance The Mapping the Underworld Project. Proc. of 12th  
 808 International Conference on Ground Penetrating Radar (GPR2008), Birmingham, UK, 16-19  
 809 June.  
 810 Romanoff, M. (1964). "Exterior Corrosion of Cast- Iron Pipe." Journal- American Water  
 811 Works Association **56**(9): 1129-1143.  
 812 Russell, D. and A. Parker (1979). "Geotechnical, mineralogical and chemical interrelationships  
 813 in weathering profiles of an overconsolidated clay." Quarterly Journal of Engineering Geology  
 814 and Hydrogeology **12**(2): 107-116.  
 815 Schmidt, A.M. (2007). Physiochemical changes in London clay adjacent to cast iron pipes.  
 816 PhD, University of Birmingham.  
 817 Schmidt, A.M., D.N. Chapman and C.D.F. Rogers (2006). Physiochemcial changes in London  
 818 Clay adjacent to cast iron pipes. Proceedings of the International Association of Engineering  
 819 Geology and the Environment conference, London, UK.  
 820 Schwertmann, U. (1991). "Solubility and dissolution of iron oxides." Plant and soil **130**(1-2):  
 821 1-25.  
 822 Sim, J.J., S.K. Bhandari, N. Smith, J. Chung, I.L.A. Liu, S.J. Jacobsen and K. Kalantar-Zadeh  
 823 (2013). "Phosphorus and Risk of Renal Failure in Subjects with Normal Renal Function." The  
 824 American Journal of Medicine **126**(4): 311-318.  
 825 Tajudin, S.A.A. (2012). Electrokinetic Stabilization of Soft Clay. PhD Thesis, University of  
 826 Birmingham, UK.  
 827 Terzaghi, K., R.B. Peck and G. Mesri (1996). Soil Mechanics in Engineering Practice, Wiley.  
 828 Tran, Anh P. and S. Lambot (2015). Development of Intrinsic Models for Describing Near-  
 829 Field Antenna Effects, Including Antenna-Medium Coupling, for Improved Radar Data  
 830 Processing Using Full-Wave Inversion. Civil engineering applications of ground penetrating

831 radar. A. Benedetto and L. Pajewski. New Delhi, India, Springer International Publishing: 227-  
832 246.

833 Van Dam, R.L. and W. Schlager (2000). "Identifying causes of ground- penetrating radar  
834 reflections using time- domain reflectometry and sedimentological analyses." Sedimentology  
835 **47**(2): 435-449.

836 Veleva, L. (2005). Soils and Corrosion. Corrosion Tests and Standards: Application and  
837 Interpretation. R. Baboian, ASTM International, OH. **2nd Edition**: 387-404.

838 Venkatramaiah, A.V. (2000). Geotechnical Engineering, Universities Press.

839 von Wolzogen Kühr, C. and L. Van der Vlugt (1964). Graphitization of cast iron as an  
840 electrobiochemical process in anaerobic soils. Maryland, USA, US Army Biological Labs  
841 Frederick MD.

842 WSAA (2003). Common Failure Modes in Pressurised Pipeline Systems. Australia, Water  
843 Services Association of Australia: 7.

844 Yong, R.N. and C.N. Mulligan (2003). Natural attenuation of contaminants in soils, CRC Press.

845

846

	Description	Chemical composition (Content %) <sup>2</sup>	Mineralogical composition (Content %) <sup>2</sup>	Physical and Chemical Properties				
				Liquid Limit	Plastic Limit	pH	Specific Gravity	Conductivity
Kaolin Clay	Clay mineral consists of an isometrical 1:1 aluminosilicate layer formed by an alumina octahedral sheet fused to a silica tetrahedral sheet connected to the other layers by hydrogen bonding. It has no exchangeable cations as it has near zero isomorphic substitution and cationic vacant. It has a chemical inertia property caused by its structure. <sup>1</sup> Kaolinite dissolves and precipitates reversibly with a thermodynamic equilibrium at 25°C. It forms through weathering of potassium feldspar and muscovite mica existed in rocks such as granite. <sup>2</sup>	SiO <sub>2</sub> (42.2) Al <sub>2</sub> O <sub>3</sub> (30.8) K <sub>2</sub> O (2.85) Fe <sub>2</sub> O <sub>3</sub> (1.11) MgO (0.28) P <sub>2</sub> O <sub>5</sub> (0.13) Rb <sub>2</sub> O (0.119) TiO <sub>2</sub> (0.082) SrO (0.045) MnO (0.034) ZrO <sub>2</sub> (0.024) CuO (0.017) As <sub>2</sub> O <sub>3</sub> (0.01)	Kaolin (66) Feldspar (6) Quartz (1) Mica (23) Montmorillonite (2)	55.6%	23.6%	5.63	2.6	37.6 µs/cm
Oxford Clay	It formed from a marine sedimentary rock from the Jurassic period and underlies much of southeast England, around Oxford, Peterborough and Weymouth. <sup>2</sup> Oxford Clay generally consists of clay minerals which make it more liable to weathering compared to the clastic clay minerals.	SiO <sub>2</sub> (34.9) Al <sub>2</sub> O <sub>3</sub> (12.6) CaO (9.68) Fe <sub>2</sub> O <sub>3</sub> (7.11) SO <sub>3</sub> (5.05) K <sub>2</sub> O (3.09) TiO <sub>2</sub> (1.23) MgO (1) Na <sub>2</sub> O (0.27) P <sub>2</sub> O <sub>5</sub> (0.27) BaO (0.15) ZrO <sub>2</sub> (0.071) V <sub>2</sub> O <sub>5</sub> (0.061) SrO (0.06) ZnO (0.029) Rb <sub>2</sub> O (0.021)	Near-illite (21) Illite-smectite (15) Quartz (28) Calcite (12) Kaolinite (7) Feldspar (4) Gypsum (3) Pyrite (2) Chlorite (3)	65.1%	35.2%	7.31	2.6	25.2 µs/cm

849 Table 2: List of input values into the FDTD simulations in relation to the soil, measured by TDR during the lab  
850 experiments

Parameter (Unit)	Type of Soil	Specification	Values <sup>1</sup> (Average)	Note
Permittivity (ε)	Kaolin Clay	2-week	31.57-53.69 (29.95)	With cast iron disc
		4-week	31.53- 34.56 (32.95)	
		3-month	34.01-36.50 (35.33)	
		2-week	33.92-33.29 (33.41)	Without the cast iron disc
		4-week	32.85- 31.09 (32.23)	
	Oxford Clay	2-week	26.11-31.44 (28.84)	With cast iron disc
		4-week	28.97	
		3-month	21.57	
		2-week	31.44-32.94 (32.38)	Without the cast iron disc
		4-week	34.65-34.01 (34.07)	
Conductivity (mS/m)	Kaolin Clay	2-week	15-127.4 (61.3)	With cast iron disc
		4-week	13.64-154.15 (62.56)	
		3-month	22.93- 409.50 (165.75)	
		2-week	7.53-85.33 (47.06)	Without the cast iron disc
		4-week	8.40-87.27 (48.62)	
	Oxford Clay	2-week	124.16-179.99 (160.0)	With cast iron disc
		4-week	126.6- 276.79 (191.2)	
		3-month	215.34-441.96 (350.29)	
		2-week	52-54.07 (53.16)	Without the cast iron disc
		4-week	58.98-66.75 (62.28)	

<sup>1</sup>Range of values are related to the distance away from disc

855    **10   List of Tables**

856	Table 1: Description and characteristics of Kaolin Clay and Oxford Clay .....	27
857	Table 2: List of input values into the FDTD simulations in relation to the soil, measured by	
858	TDR during the lab experiments.....	28

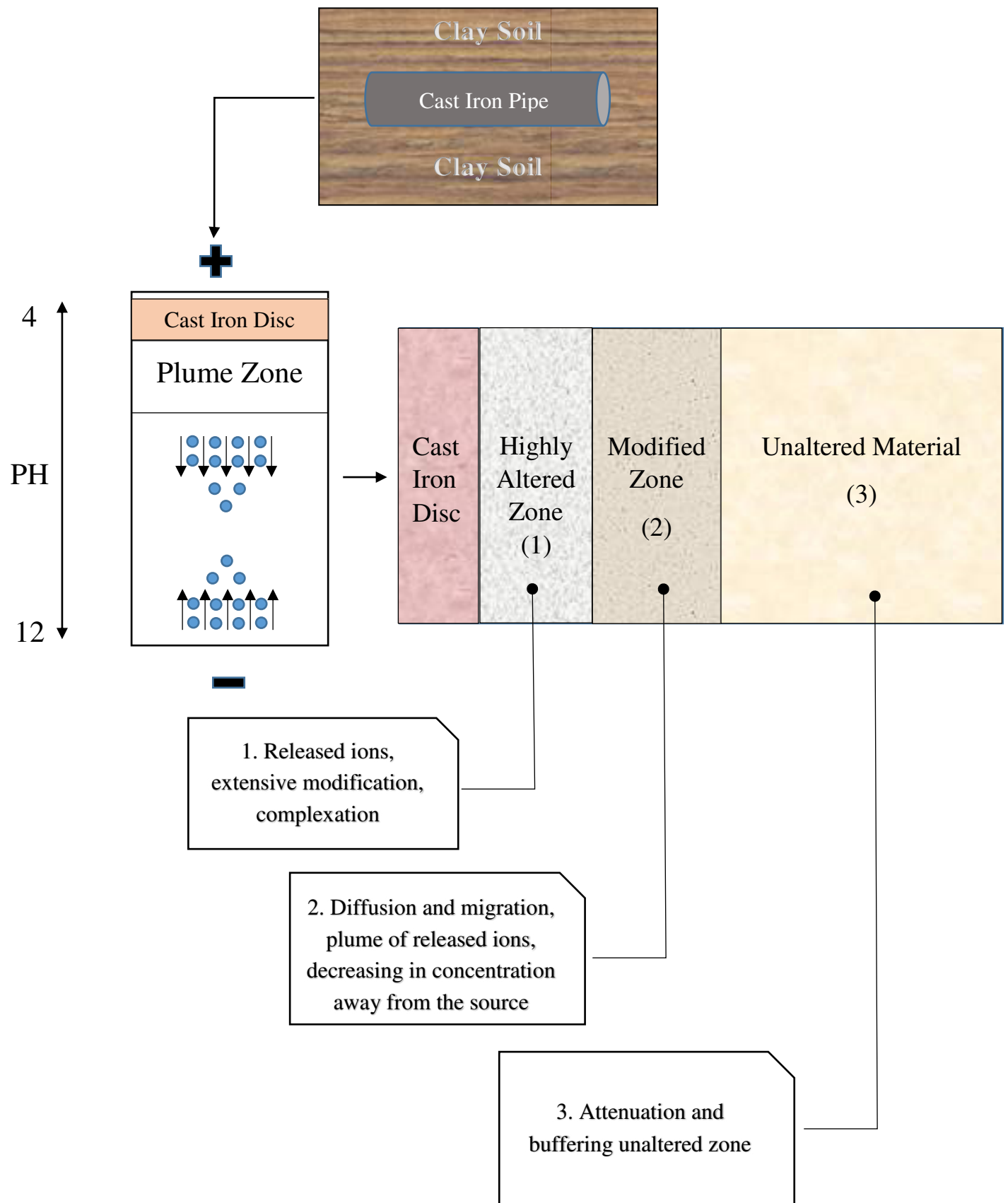


**Figure 1: Soil modifications through ion migration**

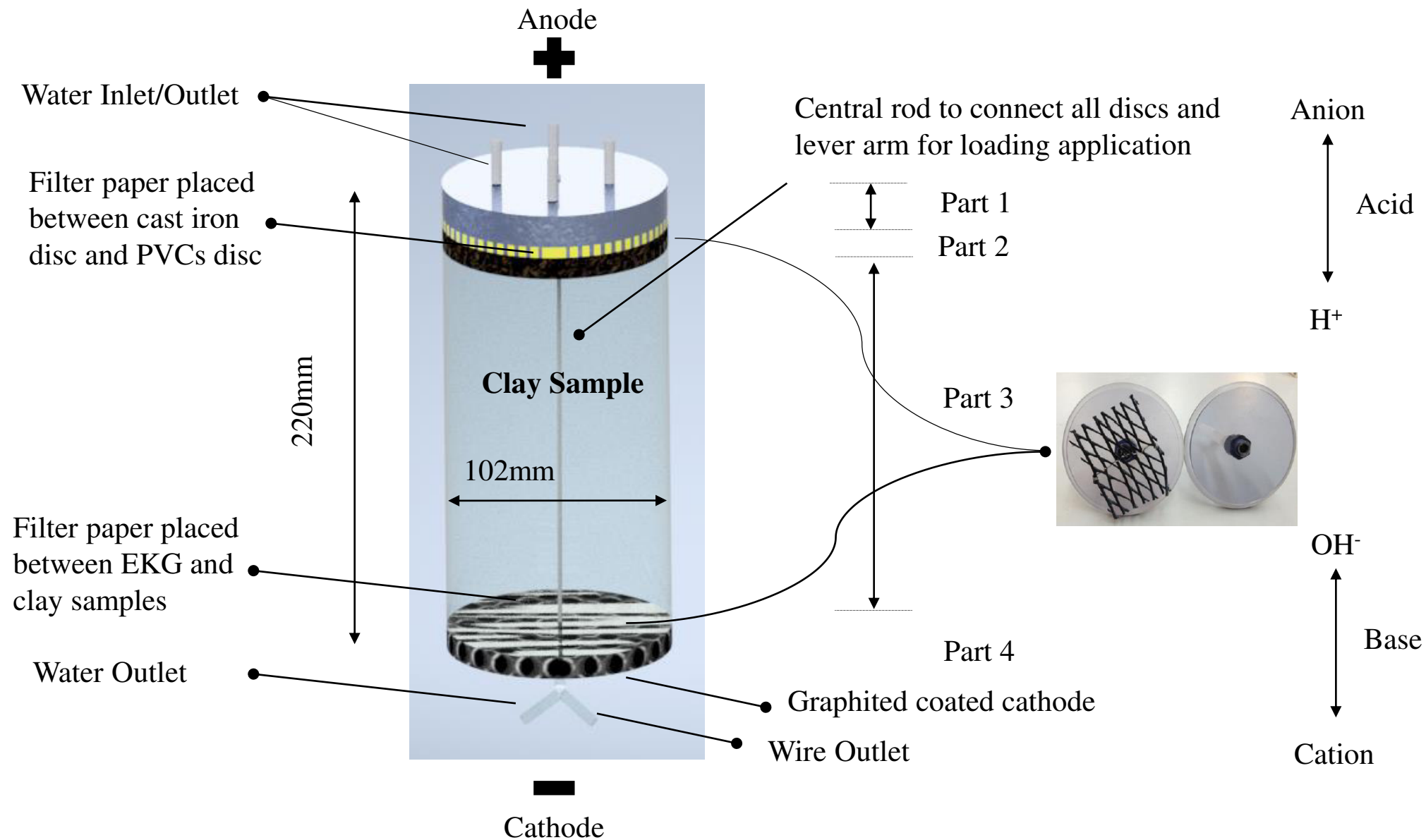


**Figure 2: Arrangement of the accelerated corrosion apparatus utilised in the experiments**



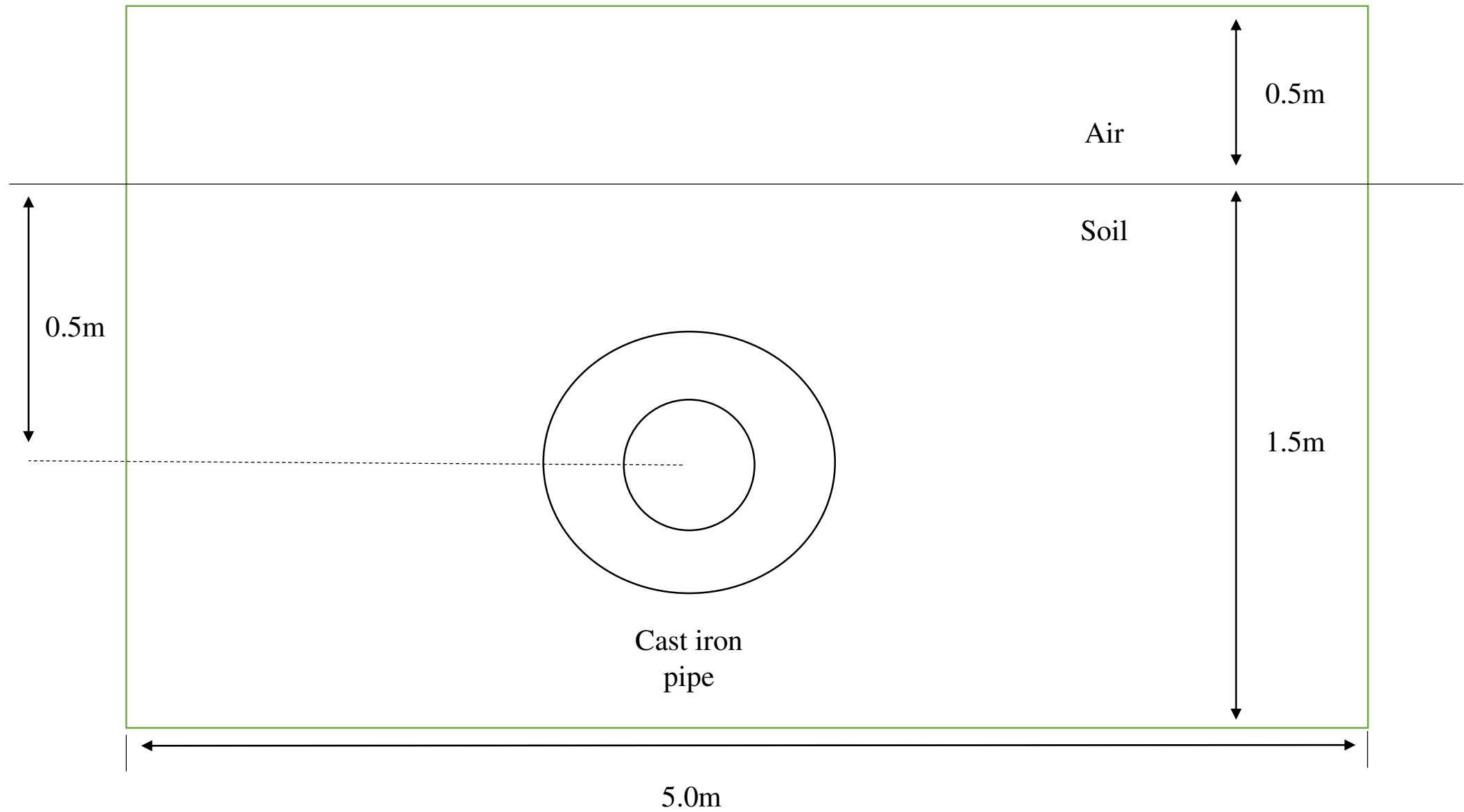


**Figure 3: The GPR model used in GPRMax**

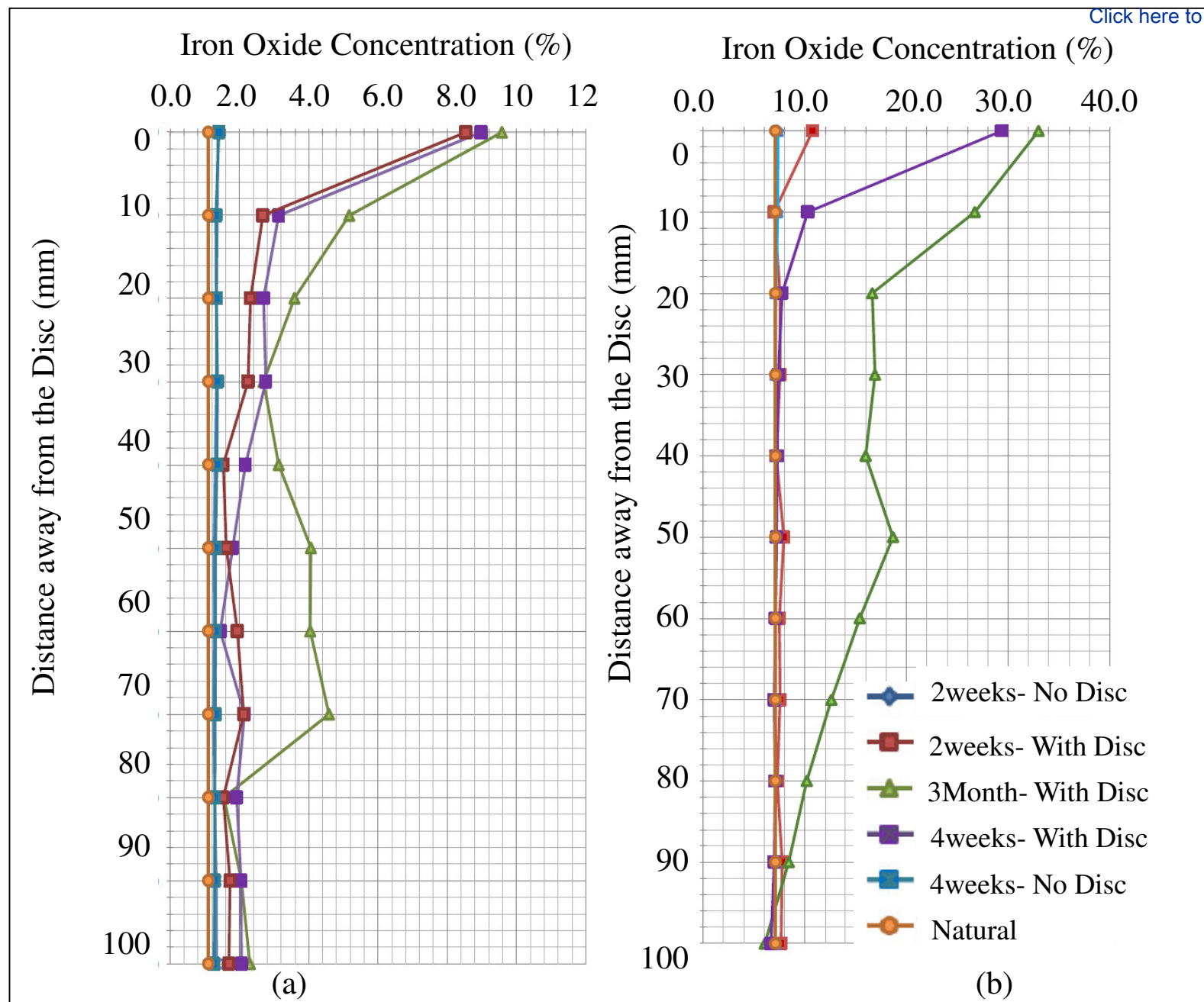


**Figure 4: Iron concentration results for (a) Kaolin Clay and (b) Oxford Clay samples**

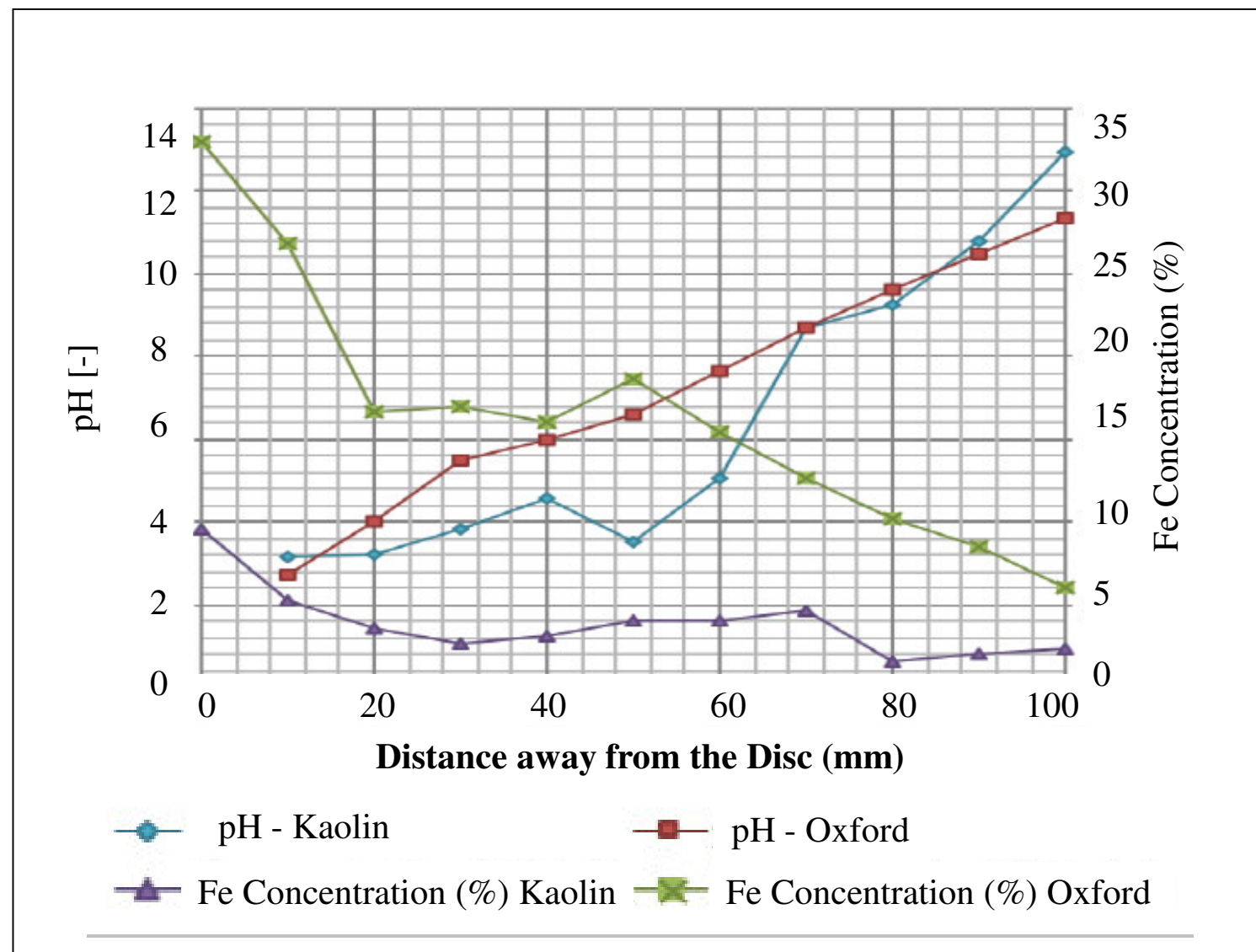


**Figure 5: pH and iron concentration results for Kaolin Clay and Oxford Clay for the 3-month samples with a cast iron disc**

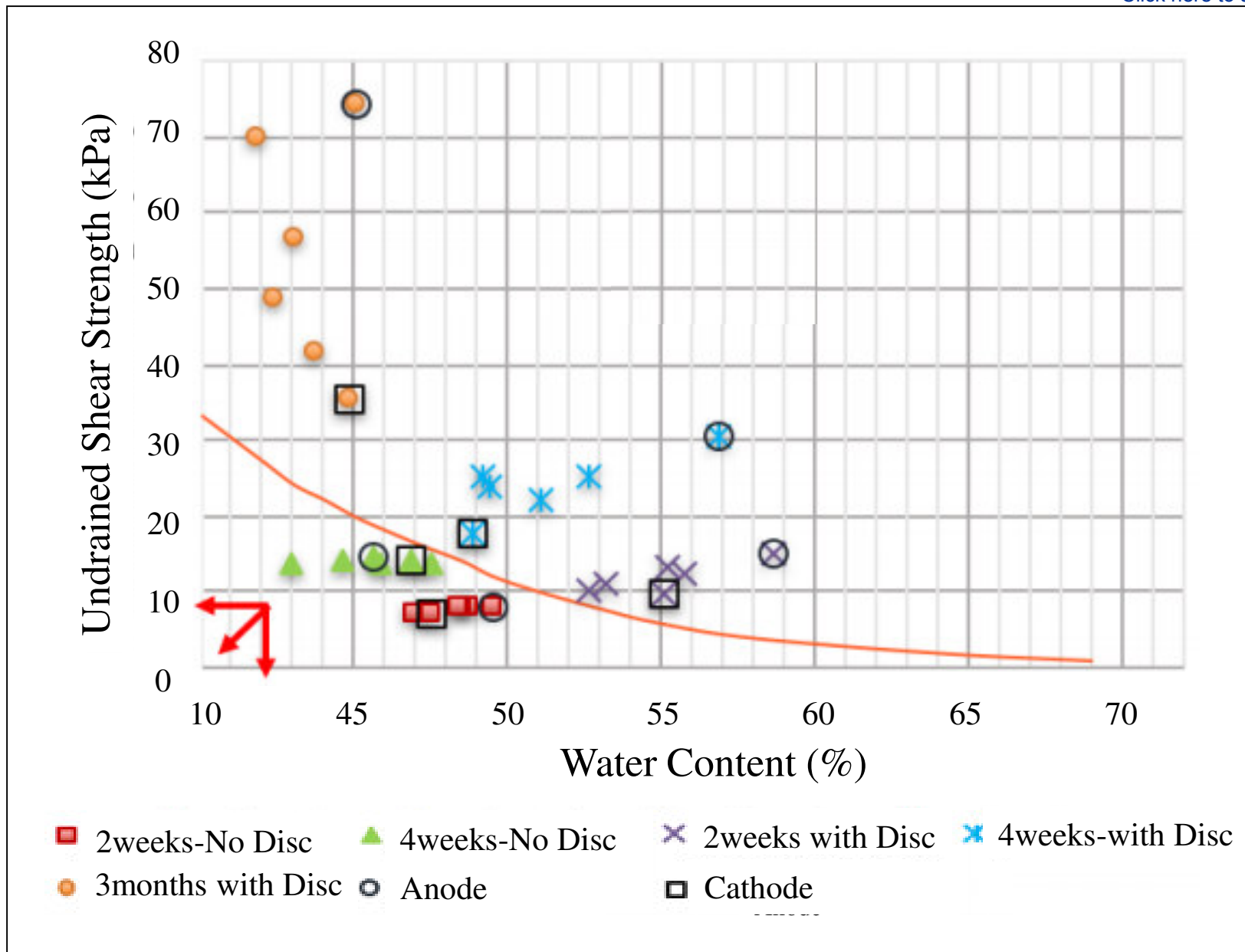


**Figure 6: Variation of soil undrained shear strength (kPa) with water content (%) for Kaolin Clay**

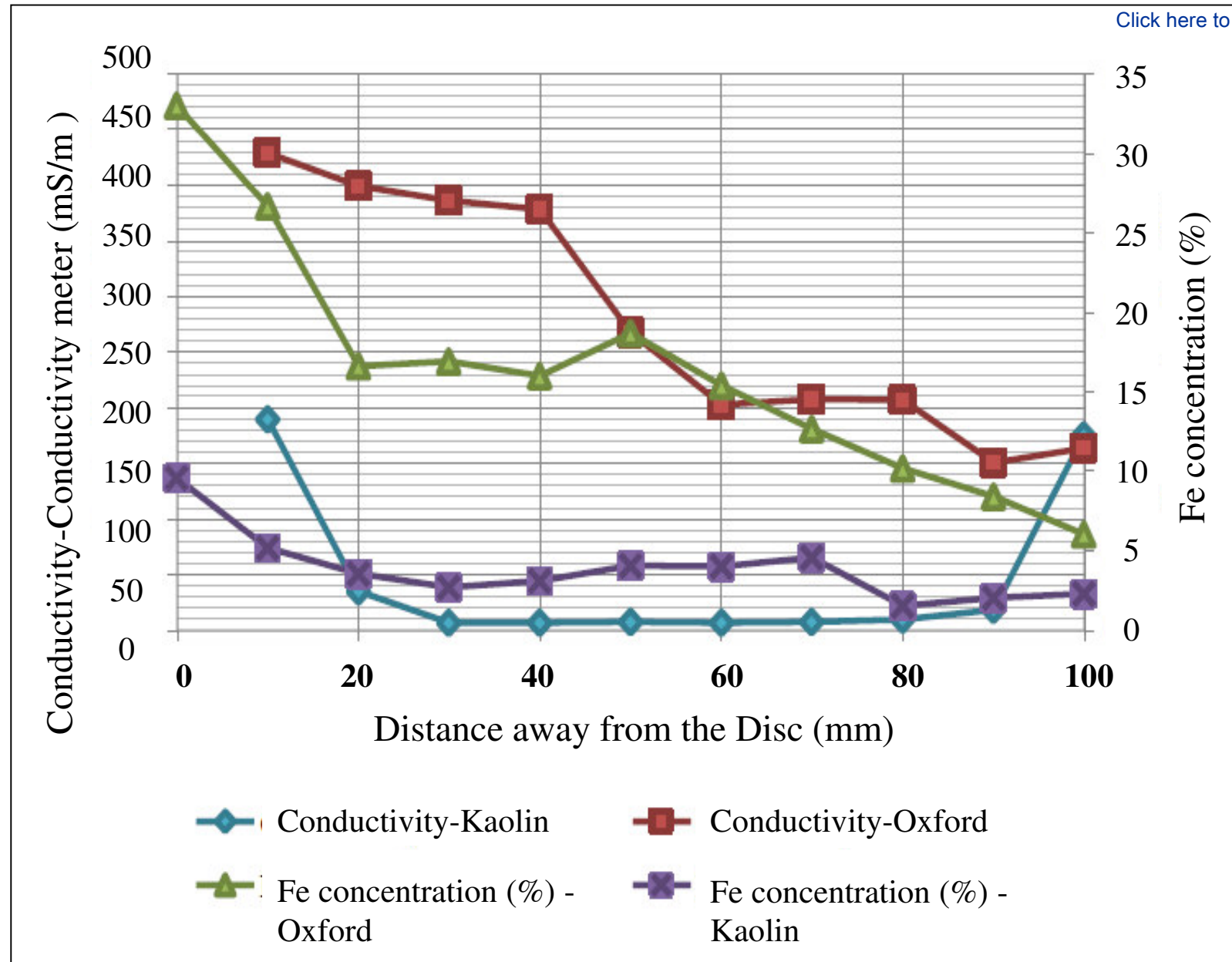


**Figure 7: Conductivity and iron concentration results for Kaolin Clay and Oxford Clay with a cast iron disc**

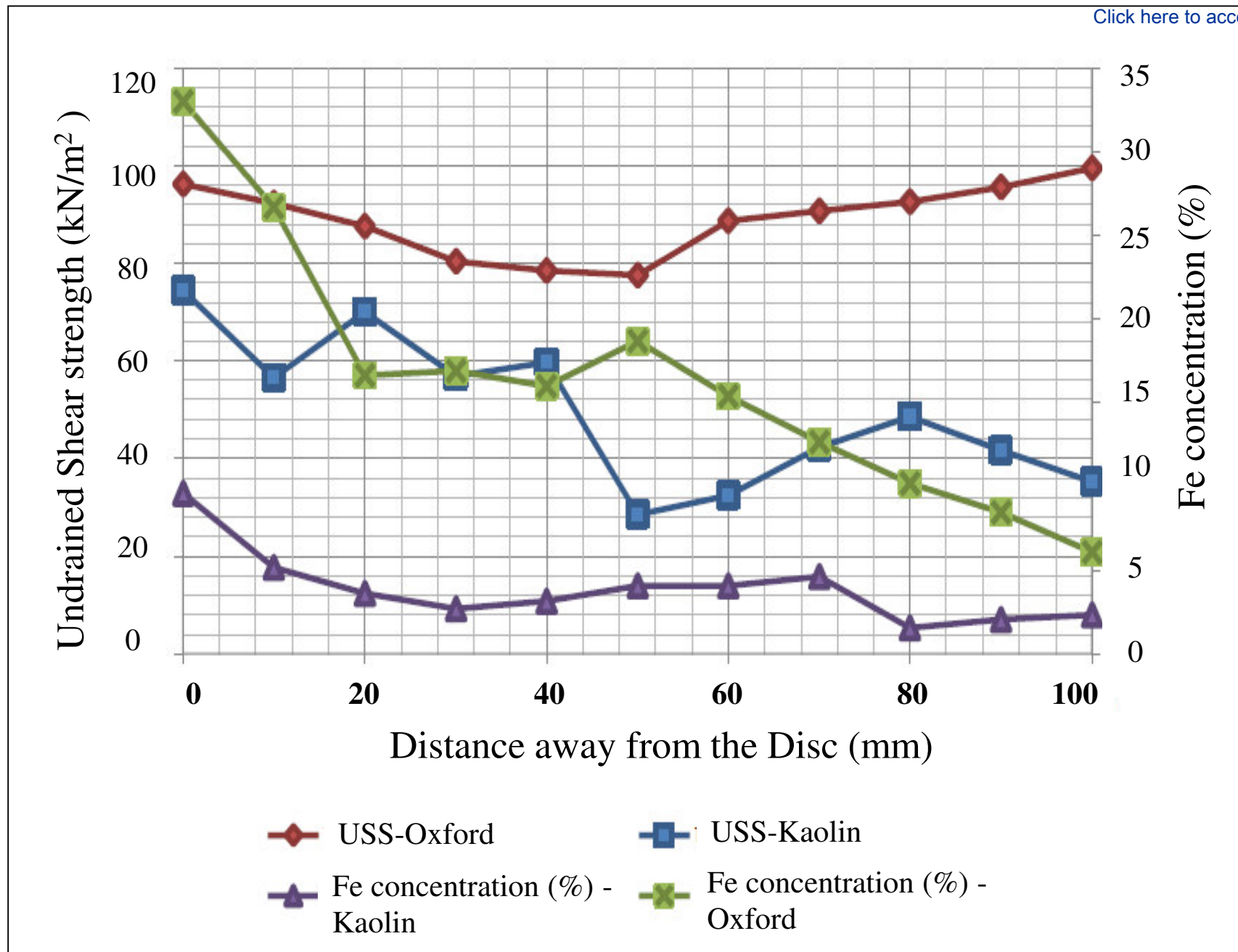


**Figure 8: Undrained shear strength (USS) and iron concentration results for Kaolin Clay and Oxford Clay for the 3-months samples with a cast iron disc**

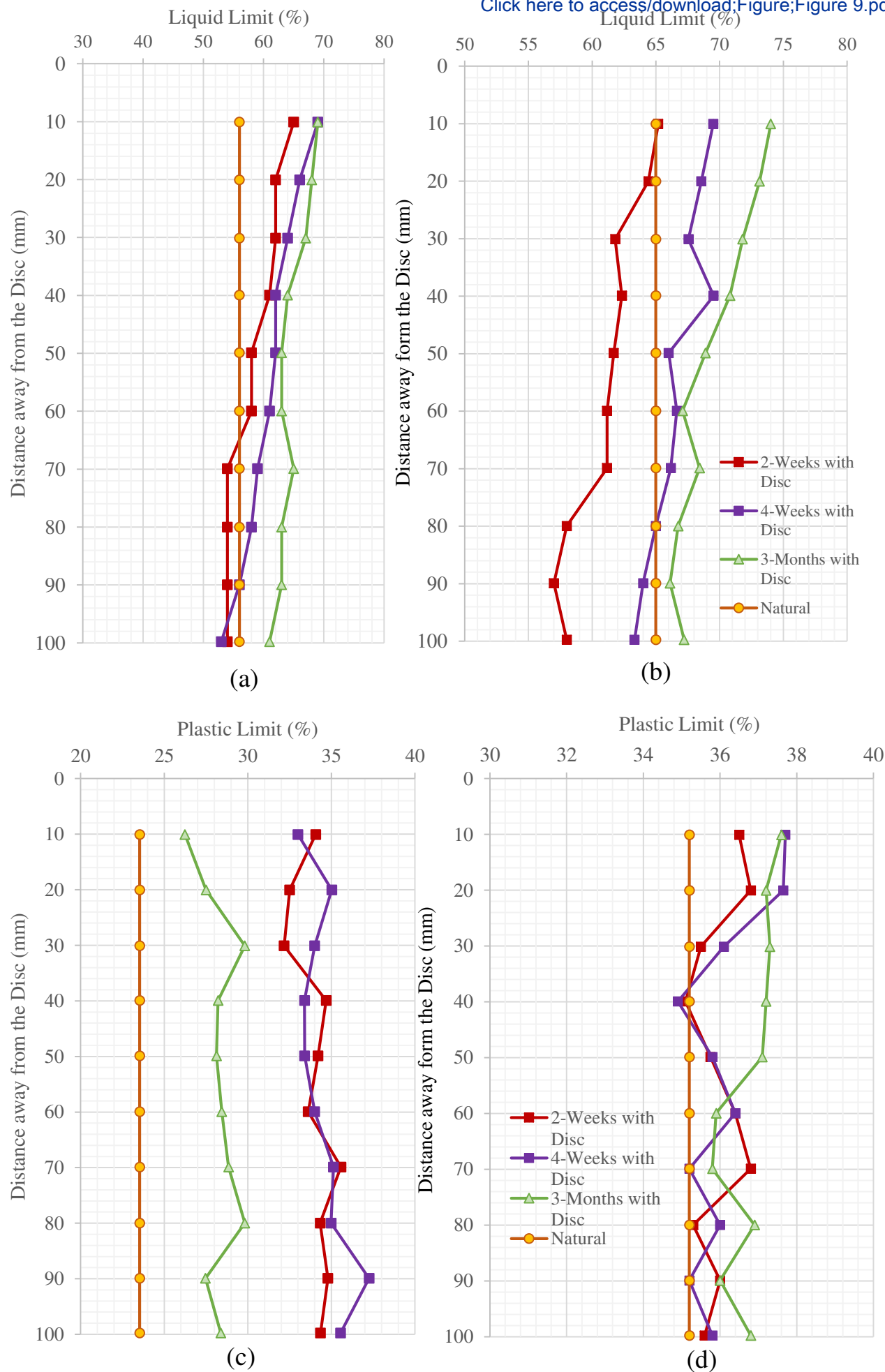


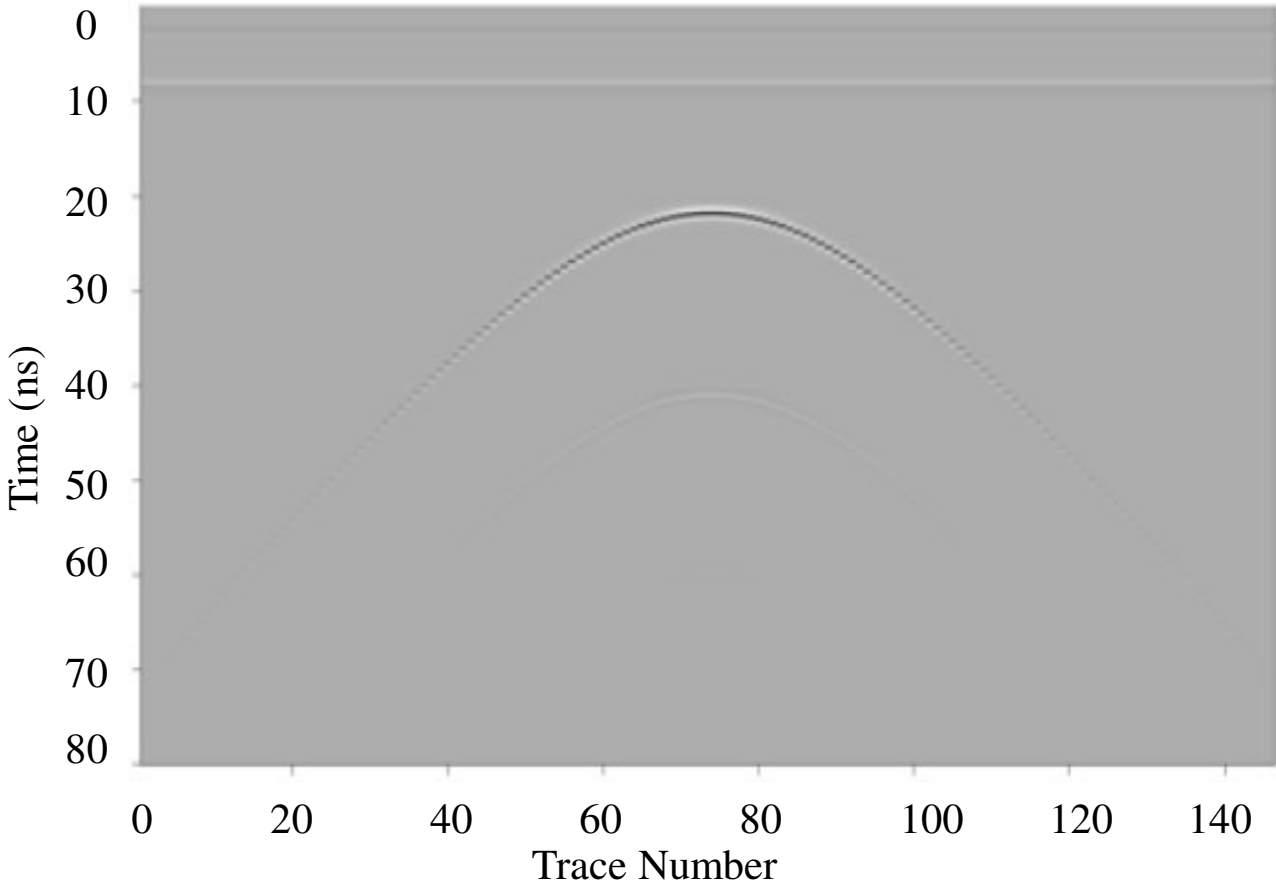
Figure 9: Liquid Limits for (a) Kaolin Clay and (b) Oxford Clay, and Plastic Limits for (c) Kaolin Clay and (d) Oxford Clay samples at different test durations



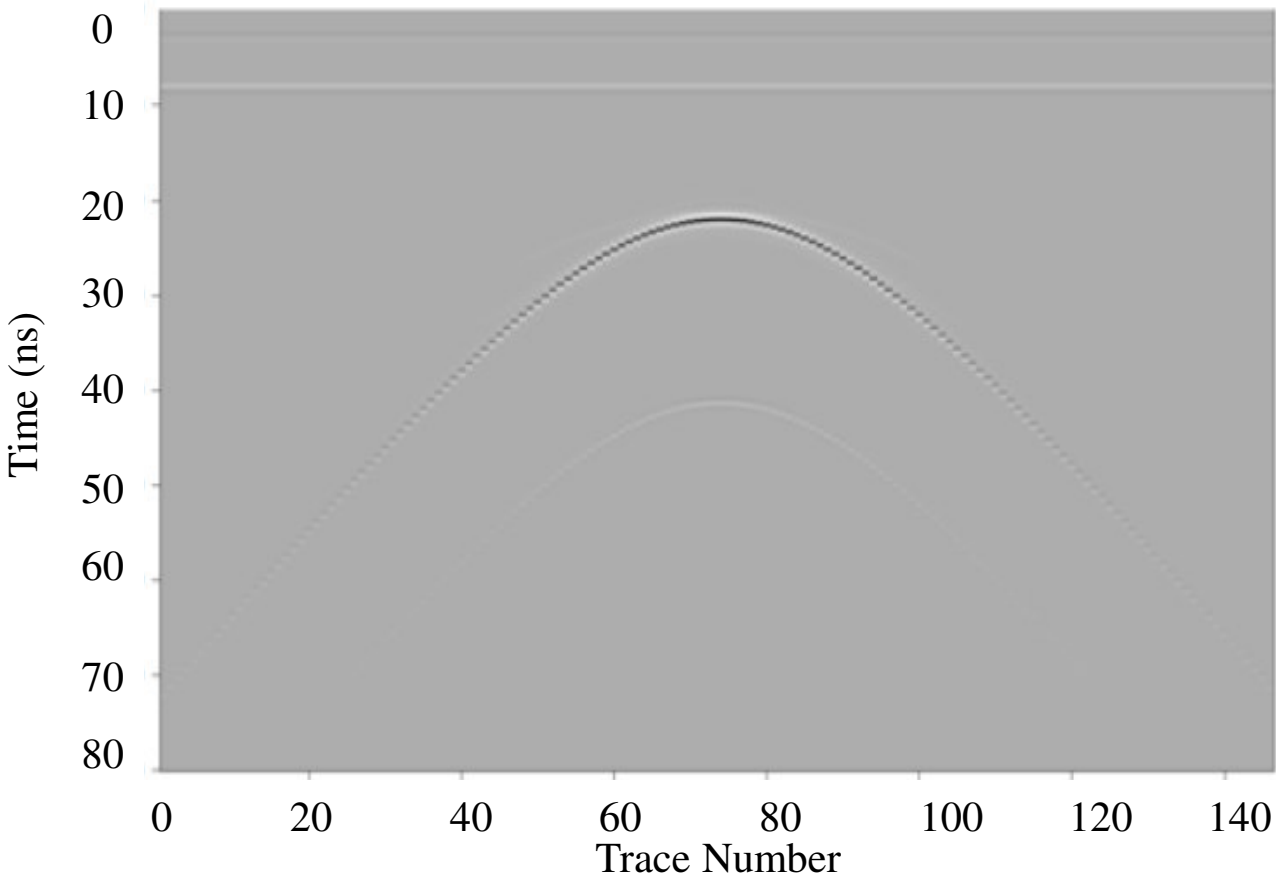


**Figure 10: Cast iron discs removed at the end of the 3-months test for the Oxford Clay (left) and the Kaolin Clay (right)**





(a)



(b)

**Figure 11: FDTD simulation using GPRMax utilising the measured test soil parameters for the Kaolin Clay with a cast iron disc at (a) 4-weeks, (b) 3-months**

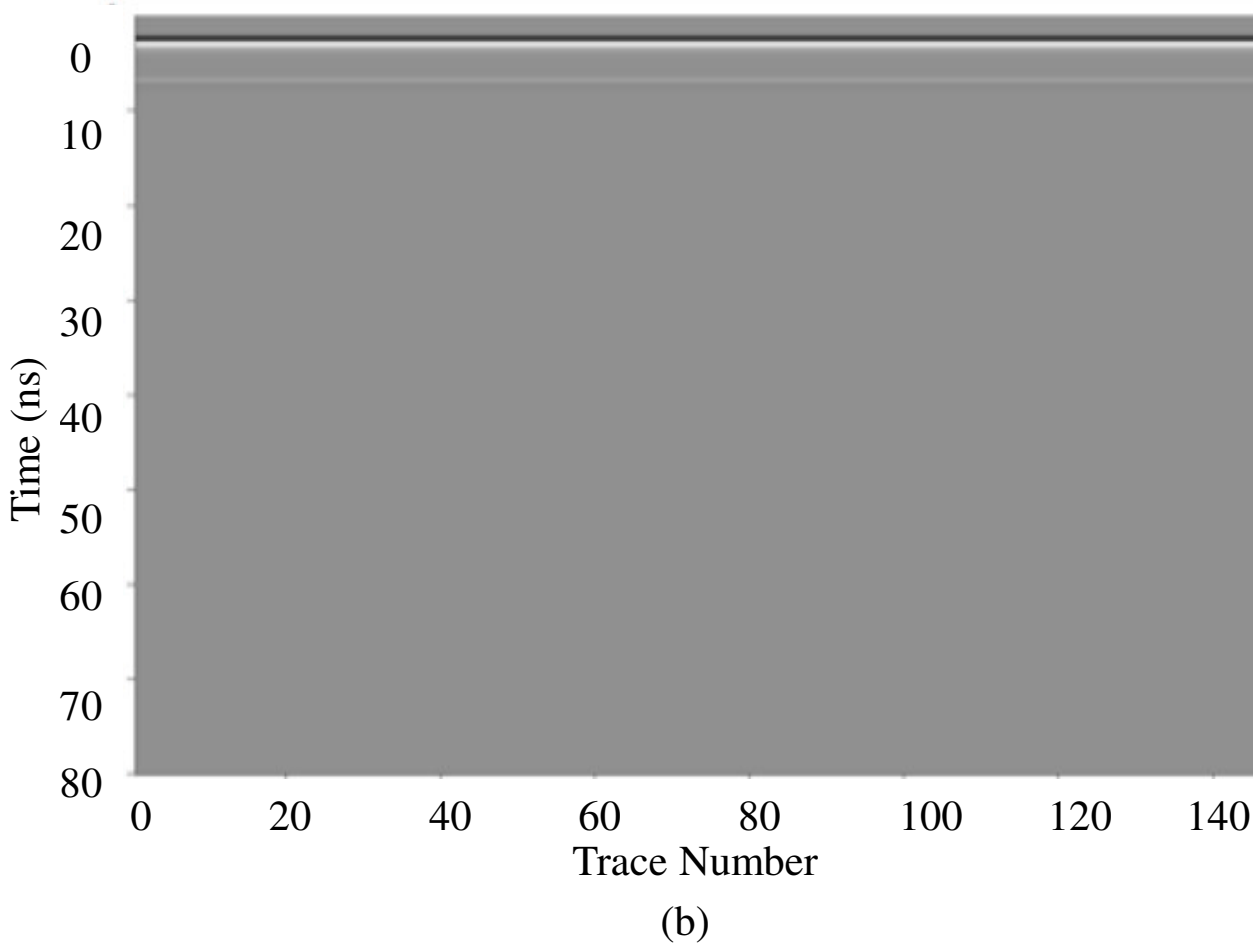
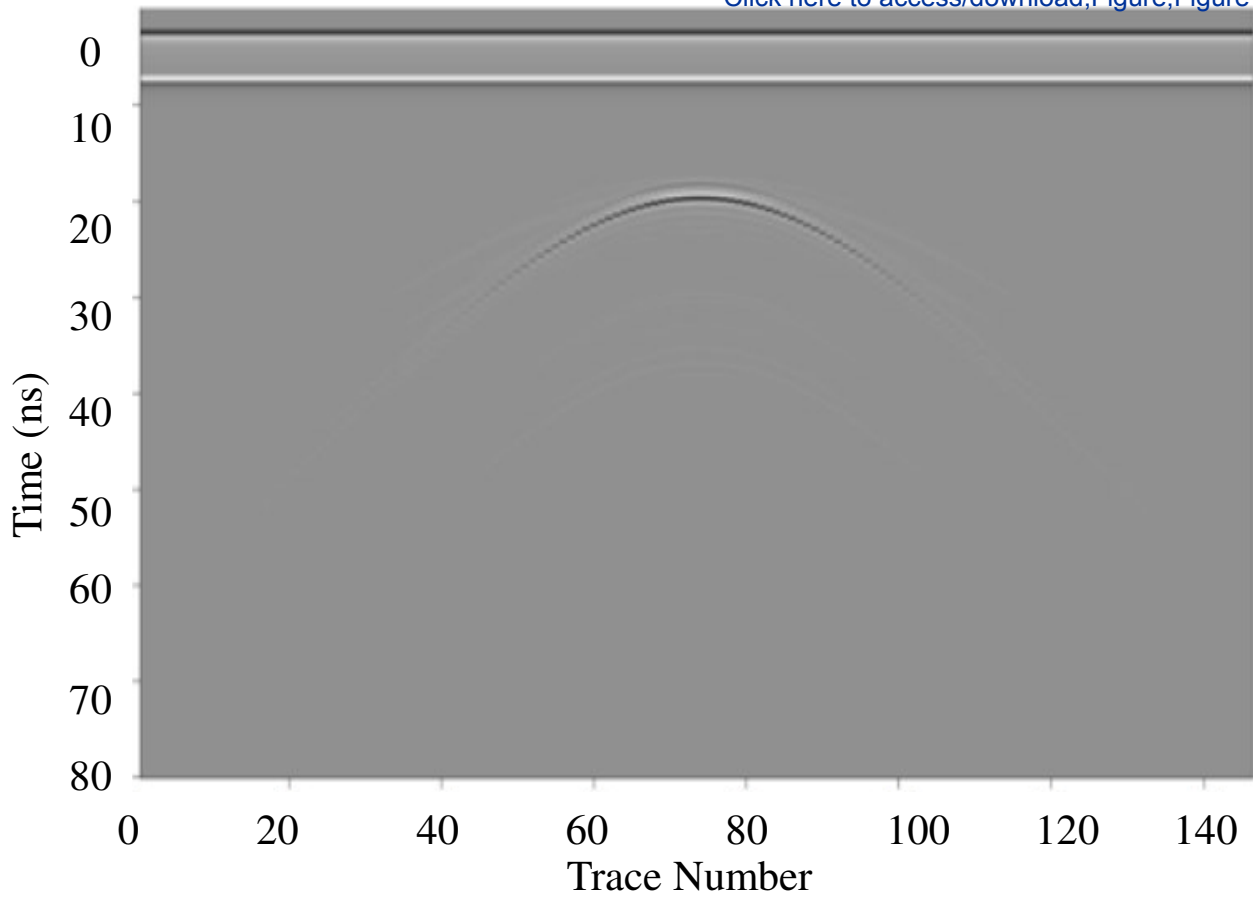
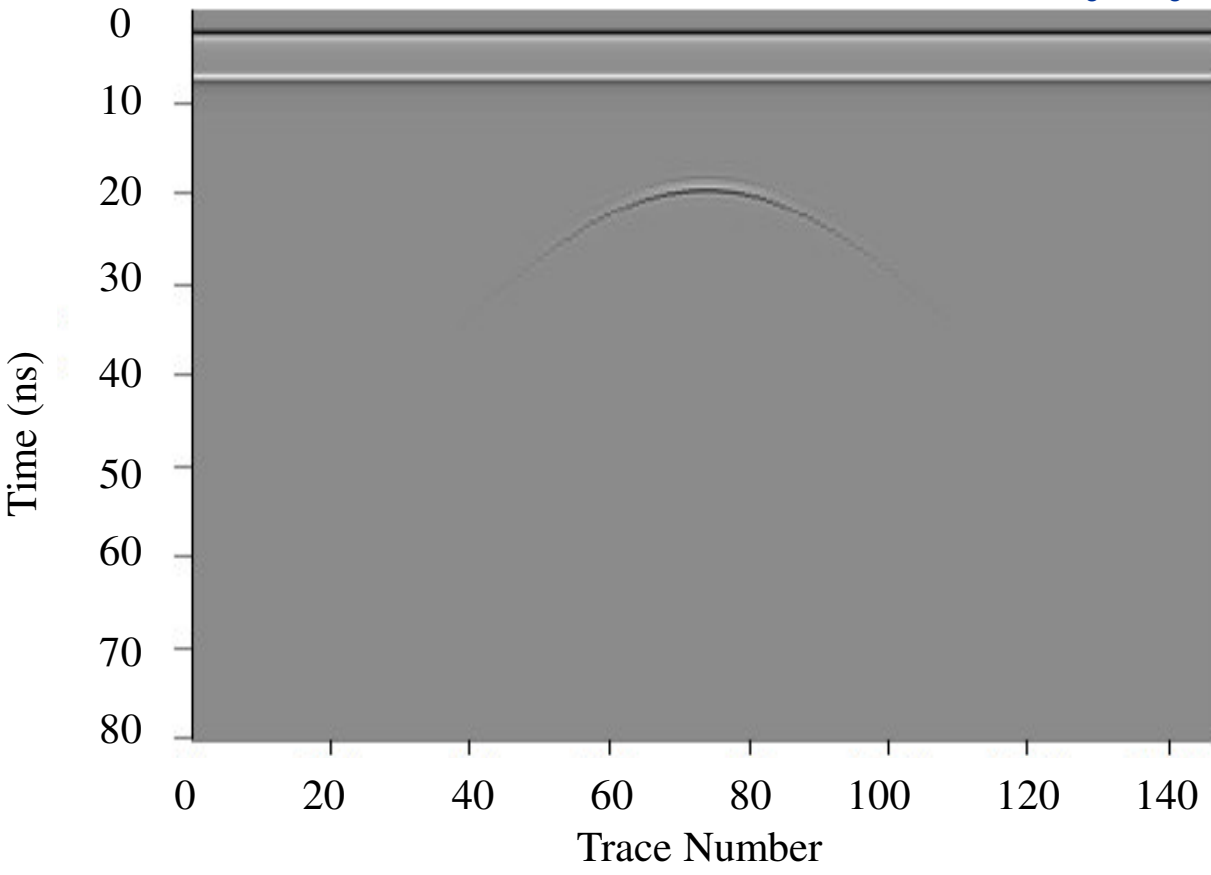
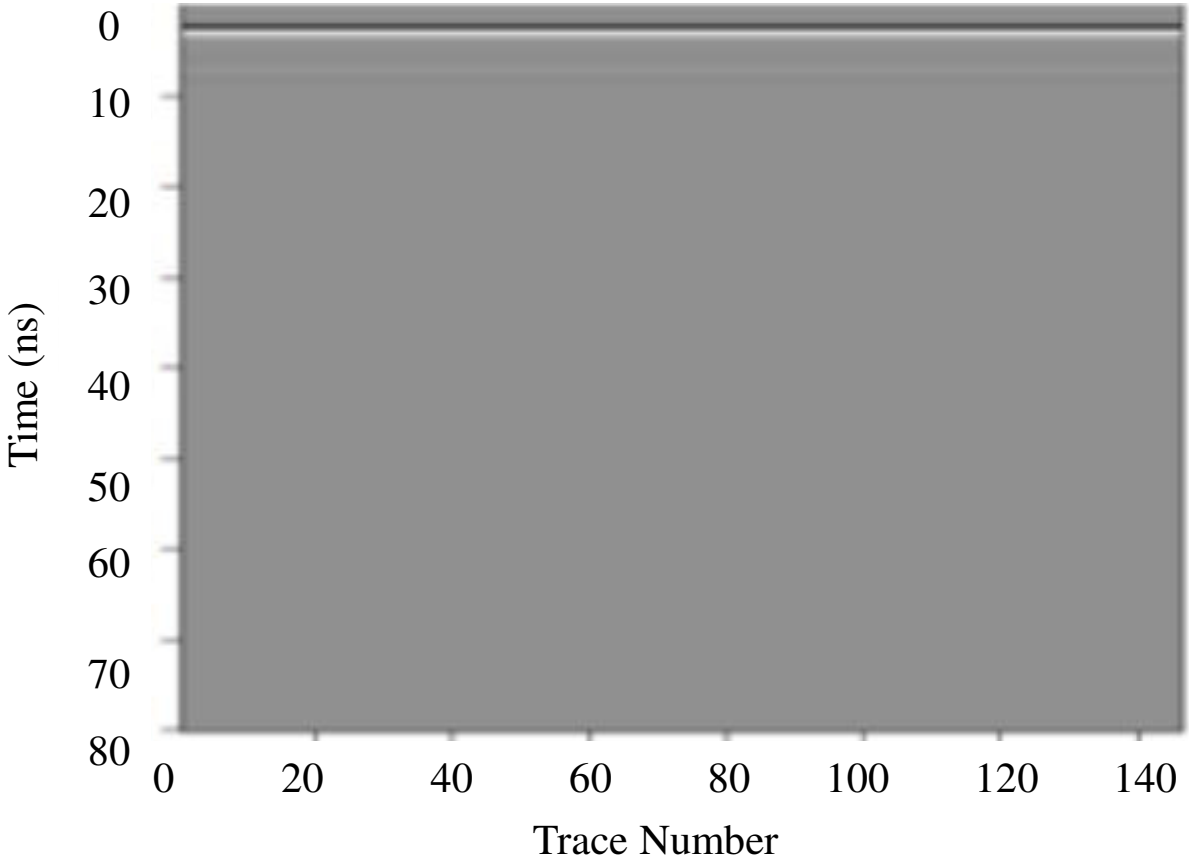


**Figure 12: FDTD simulation using GPRMax utilising the measured test soil parameters for the Oxford Clay with a cast iron disc at (a) 4-weeks and (b) 3-months**



(a)



(b)

**Figure 13: FDTD simulation using GPRMax utilising the interpolated test soil parameters for the Oxford Clay with a cast iron disc at (a) 7-weeks and (b) 9-weeks**